

On a third S -matrix in the theory of quantized fields on curved spacetimes

Hanno Gottschalk[#] and Thomas Hack^ᵇ

December 2, 2024

^ᵇ: Physikalisches Institut, Rheinische Friedrich-Wilhelms-Universität Bonn

[#]: Institut für angewandte Mathematik, Rheinische Friedrich-Wilhelms-Universität Bonn

Abstract: Wightman functions for interacting quantum fields on curved space times are being calculated via the perturbation theory of the Yang-Feldman equations, where the incoming field is a free field in a quasifree representation. We show that these Wightman functions that are obtained as a sum over extended Feynman graphs fulfill the basic axioms of hermiticity, invariance, spectrality (on stationary spacetimes), perturbative positivity and locality (the latter property is shown up to second order in the loop expansion). In the case of non-stationary spacetimes, the outgoing field in general is in a non-quasifree representation of the CCR. This makes it necessary to develop a method to calculate the unitary transformation between a non-quasifree representation and a quasifree one. This is carried out using \star -calculus on the dual of the Borchers algebra with a combinatorial co-product. Given that preferred quasifree representations for early and late times exist, we thus obtain a complete scattering description using three S -matrices: The first is determined by vacuum expectation values between incoming and outgoing fields. The second is a unitary transformation between the non-quasifree representation of the "out"-fields and the quasifree representation for the "in"-field. The last one is the Bogoliubov transformation between the preferred representation at early times (i.e. the "in"-field representation) and the preferred representation at late times.

Key words: *Interacting quantum fields on curved spacetimes, Wightman functions, perturbation theory, non-quasifree CCR representations*

MSC (2000): 81T20

1 Introduction

In the theory of quantum fields on curved spacetimes it has been realized quite early that interactions contribute quite significantly to particle production due to non-stationary gravitational

forces [3]. Thus the scattering theory of interacting fields on physical backgrounds was in the focus of attention. The picture that has been drawn is that this scattering behavior is essentially governed by two S -matrices. One is the known scattering matrix from quantum fields in flat space time that can be calculated with the help of the Lehmann-Symanzik-Zimmermann (LSZ) method. The second scattering matrix is the S -matrix originating from a Bogoliubov transformation between "in"- and "out"-representations that are both quasifree but not the same. The latter S -matrix has been well-known from the theory of free quantum fields on curved spacetimes.

With some exceptions, e.g. [4], that however have not been very precise on the topic of asymptotic conditions either, most of these works [1, 2, 3, 5] assumed asymptotic conditions for the interacting field in the Heisenberg picture $\phi(x) \rightarrow \phi^{\text{in}/\text{out}}(x)$ as $x^0 \rightarrow \mp\infty$ where $\phi^{\text{in}} = a(x) + a^\dagger(x)$ and $\phi^{\text{out}} = b(x) + b^\dagger(x)$ with $a(x)$, $a^\dagger(x)$ and $b(x)$, $b^\dagger(x)$ annihilation and creation fields s.t. $a(x)\Omega^{\text{in}} = b(x)\Omega^{\text{out}} = 0$ for suitable "in"- and "out"-Fock vacuum states. It seems however that this sort of asymptotic condition has never been checked. In fact, once the "in"-state for the field has been specified to be a certain, say, quasifree state, the field theory is determined by these initial conditions and the equations of motion. Thus properties of "out"-fields have to be derived and cannot be assumed ab initio. In [11] this question has been investigated for a sort of QFT toy model on curved spacetimes which failed to reproduce the assumption of quasifreeness of the outgoing state.

In the present work we show that this is not an artefact of the toy model, but occurs genuinely in quantum field theory on non-stationary spacetimes. In order to be able to access this question, one has to calculate the representation of the outgoing field. This of course is not possible using commutative scattering amplitudes from LSZ or Feynman path integral formalisms, but one has to calculate the vacuum expectation values (Wightman functions) of the non-commutative quantum theory. Such a formalism of a perturbative calculation of Wightman functions is readily available on Minkowski spacetime [17, 20, 21]: The sectorized Feynman graph formalism of Ostendorf and Steinmann has the merit to eliminate all unnecessary assumptions from the formalism, in particular the canonical commutation relations (CCR) and initial conditions. While this is advantageous for Minkowski spacetime, it however poses a problem for curved spacetimes as there initial conditions should matter.

Here we therefore develop an independent formalism to calculate the Wightman functions for quantum fields on curved spacetimes using a quasifree "in"-representation and the perturbation theory of Yang-Feldman equations, cf. Section 2. We then develop a Feynman graph calculus for the Wightman functions where the external vertices of the Feynman graph have to be labeled properly and the edges have to be decorated with arrows symbolizing various kinds of propagators (Section 3). The basic properties of the Wightman functions are then described in the Sections 4 and 5. While Hermiticity, invariance under orthochronous isomorphisms, perturbative positivity and, in the case of stationary spacetimes, spectrality do not pose major problems, the proof of locality requires quite a bit of combinatorial efforts. We give the proof to the second order in the loop expansion only, however we retain that the essential elements of a complete proof to all orders become visible. Even for the Minkowski spacetime, where locality can be proven with the help of the split property of time ordered products and Lorentz invariance [17], our hands-on approach might give some instructive insight into "locality at work".

In Section 6 the Klein-Gordon equation and the CCR are verified for the "out"-field. The proof of the CCR is similar to the one of locality and holds to second order in the loop expansion. It is also verified that the "out"-field representation is genuinely non-quasifree. This poses the

question how to interpret such non-quasifree representations. In the case of unitary equivalence with a quasifree representation, we give a complete solution to this problem using \star -calculus on the dual of the Borchers algebra with a combinatorial co-product (Section 7). It turns out in Section 8 that the compete scattering description is most conveniently given in terms of three distinct S -matrices. The first one is the S -matrix due to the quantum scattering between the "in"-particle space and the GNS-space of the non-quasifree representation of the "out"-field. The second S -matrix, which is the new one, is obtained by calculating the particle content of the "out"-GNS-vacuum in the "in"-Fock space. Finally, to obtain the particle content of states in a preferred, quasifree "out"-representation, we have to use the Bogoliubov S -matrix [22].

Some technical parts on the multiplicity of graphs, the two loop calculation and \star -calculus are given in the Appendices A–C.

All calculations are carried through in non-renormalized perturbation theory. This is mostly due to the fact that we have little to contribute to the theory of renormalization on physical backgrounds, which is now well understood with the help of the Epstein-Glaser method and microlocal analysis [7, 8, 13, 14, 15]. The simplest possible way to renormalize in the formalism given here would thus be to make contact with these works, which should not pose any principle problem as in both formalisms the equation of motion and quasifree initial conditions are assumed (adiabatic coupling constants could be introduced in this work as well). For the flat spacetime we can just refer to the equivalent formalism of Ostendorf and Steinmann, which has been properly renormalized with the BPHZ method. Let us furthermore note that the main results - locality of Wightman functions and non quasifree CCR for the out-field - hold already on the level of integrands, i.e. prior to the possibly divergent integration. As any possible regularization scheme of divergent integrals should assign zero to an zero integrand, these results hold for any renormalization prescription. It is furthermore not difficult to define a cut-off prescription that preserves all relations between the propagators that we need, e.g. a mode cut-off in the "in"-field and in the retarded and advanced propagators would do. Then all assertions of this work hold as they stand at any finite value of the cut-off.

2 Setting

We want to perturbatively calculate Wightman functions, i.e. vacuum expectation values (VEVs) of hermitian scalar fields, on a globally hyperbolic Lorentzian manifold (M, g) in ϕ^p -theory. That is, our fields satisfy the equation

$$(\square + m^2 + \kappa R)\phi = \lambda\phi^{p-1} \quad (1)$$

with coupling constant λ , scalar curvature R , mass m and $\square = \nabla_a \nabla^a$, ∇^a being the covariant derivative associated with g .

At first we introduce the fundamental functions of the theory. Let G_r (G_a) be the unique [10] retarded (advanced) fundamental solutions of the Klein-Gordon operator $(\square + m^2 + \kappa R)$, i.e. they are real valued bidistributions on M satisfying

$$(\square + m^2 + \kappa R)G_{r/a}(x, y) = \delta(x, y) \quad (2)$$

and $\text{supp}_x G_{r/a}(x, y) \subset \overline{V}_y^\pm$, \overline{V}_x^+ (\overline{V}_x^-) being the open causal forward (backward) cone with base-point x and the bar stands for the topological closure. $\delta(x, y)$ is the delta-distribution

associated with g , i.e. $\int_M \int_M \delta(x, y) f(x) f(y) d_g x d_g y = \int_M f^2(x) d_g x$, where $d_g x = \sqrt{-g} dx$, $g = \det g$, is the canonical volume form associated with g . We note that $G_r(x, y) = G_a(y, x)$ and define the antisymmetric bidistribution

$$D(x, y) = G_r(x, y) - G_a(x, y). \quad (3)$$

Obviously D fulfills the Klein-Gordon equation in both arguments and vanishes for $x \perp y$, i.e. for space-like separated x and y .

To calculate the desired Wightman functions we need to specify initial conditions for the field $\phi(x)$. We do so by postulating that for large asymptotic times $x^0 \rightarrow \mp\infty$ the local field $\phi(x)$ converges to free incoming or outgoing fields $\phi^{\text{in/out}}(x)$. For space-times (M, g) that are "large" enough to allow the fields to disperse quickly enough to become finally non-interacting, this is formulated in terms of the Yang-Feldman equations [23]

$$\phi^{\text{loc}}(x) := \phi(x) = \phi^{\text{in/out}}(x) + (G_{r/a} * j)(x), \quad (4)$$

where we formally define the convolution of a bidistribution B with a distribution w as

$$(B * w)(x) := \int_M B(x, y) w(y) d_g y \quad (5)$$

and the current j equals $\lambda \phi^{p-1}$ in our case.

It is necessary to specify a representation for $\phi^{\text{in}}(x)$ "by hand" as in absence of spectral conditions on general curved manifolds the Klein-Gordon equation and the canonical commutation relations (CCR) are not sufficient to fix the representation.

To do so, we at first define the propagators $D^\pm(x, y)$ as complex valued bi-distributions on M satisfying the Klein-Gordon equation in both arguments and $\text{Im} D^\pm = \pm \frac{1}{2} D$, $D^+(x, y) = \overline{D^+(y, x)} = D^-(y, x)$, i.e. $\tilde{D} = 2\text{Re} D^+$ is symmetric. We furthermore demand that D^+ is invariant under isometric diffeomorphisms preserving the time direction, which only constrains \tilde{D} , as D automatically fulfills that condition. Lastly we demand that D^+ is positive, i.e. $\int_M \int_M D^+(x, y) \overline{f(x)} f(y) d_g x d_g y \geq 0$ for all test functions f on M . It is well-known that the above conditions do not uniquely specify \tilde{D} . For a discussion of the existence of such (and even more general) bi-distributions see [22].

In order to obtain a particle picture for the incoming states, we specify the state for the in field as a quasifree state with two point function D^+ . \tilde{D} by our assumptions is a symmetric bidistribution that fulfills the Klein-Gordon equation in both arguments. Thus, $\tilde{D} * f$ for any test function f solves the Klein-Gordon equation and clearly $(\tilde{D} * f, \tilde{D} * h) = \int_M \int_M \tilde{D}(x, y) \overline{f(x)} h(y) d_g x d_g y$ gives a well defined scalar product on the space of complex solutions of the Klein-Gordon equation with compactly supported initial conditions. Let \mathcal{H} be the completion of this space w.r.t. $(., .)$. Likewise, the imaginary part $\frac{1}{2} D$ of D^+ defines a (\mathbb{C} -bilinear) symplectic form Σ on the space of complex valued solutions via $\Sigma(D * f, D * g) = D(f, g)$ that extends continuously to \mathcal{H} .

Upon comparison with the symplectic form, the inner product induces a complex structure J such that $\Sigma(\bar{\psi}, \chi) = (\psi, J\chi)$ for any two solutions. One easily obtains $J^* = -J$, $J^2 = -1$ and thus $J = i(K^+ - K^-)$ with K^\pm the projector on the eigenspace of J with eigenvalue $\pm i$. The spaces $\mathcal{H}^\pm = K^\pm \mathcal{H}$ are called the positive/negative frequency space, respectively. We note that $\bar{\mathcal{H}}^\pm = \mathcal{H}^\mp$ where the bar stands for complex conjugation since $J\bar{\psi} = -i\bar{\psi}$ for $\psi \in \mathcal{H}^+$.

Let \mathcal{F} be the symmetric Fock space over \mathcal{H}^+ with scalar product $\langle ., . \rangle$ and let Ω be the Fock vacuum. By $a^\dagger(\psi)$, $a(\psi)$, $\psi \in \mathcal{H}^+$, we denote the usual creation and annihilation operators on

\mathcal{F} . We use the convention $a(\bar{\psi})^* = a^\dagger(\psi)^*$, $\psi \in \mathcal{H}^+$, in order to obtain a \mathbb{C} -linear definition for $a(\chi)$, $\chi \in \mathcal{H}^-$. Here $*$ stands for taking the adjoint (neglecting domain questions). The incoming field is defined as \mathbb{C} -linear operator valued distribution

$$\phi^{\text{in}}(f) = a(K^- \tilde{D} * f) + a^\dagger(K^+ \tilde{D} * f). \quad (6)$$

In fact, by [22, Lemma 3.2.1] $(\tilde{D} * f, \tilde{D} * h) = \tilde{D}(\bar{f}, h) = \int_M \bar{f} \tilde{D} * h \, dx = \Sigma(\overline{D * f}, \tilde{D} * h) = (D * f, J\tilde{D} * h)$ for all test functions f, h , from which $-JD * f = \tilde{D} * f$ follows. Application to (6) gives $\phi^{\text{in}}(f) = ia(K^- D * f) - ia^\dagger(K^+ D * f)$ which is the definition given in [22].

On the level of truncated Wightman functions the quasifree representation can be specified as follows:

$$\langle \Omega, \phi^{\text{in}}(x) \phi^{\text{in}}(y) \Omega \rangle^T = D^+(x, y), \quad (7)$$

$$\langle \Omega, \phi^{\text{in}}(x_1) \cdots \phi^{\text{in}}(x_n) \Omega \rangle^T = 0 \quad \text{for } n \neq 2. \quad (8)$$

The truncated Wightman functions are defined via a cluster expansion as

$$\langle \Omega, \phi^{a_1}(x_1) \cdots \phi^{a_n}(x_n) \Omega \rangle = \sum_{I \in \mathcal{P}^{(n)}} \prod_{\{j_1, \dots, j_l\} \in I} \langle \Omega, \phi^{a_{j_1}}(x_{j_1}) \cdots \phi^{a_{j_l}}(x_{j_l}) \Omega \rangle^T \quad (9)$$

where $a_j \in \{\text{in, loc, out}\}$, $\mathcal{P}^{(n)}$ is the collection of all partitions of $\{1, \dots, n\}$ into disjoint, nonempty subsets $\{j_1, \dots, j_l\}$ with $j_1 < \dots < j_l$ [11]. Taking (7)-(8) into account, it follows immediately that a much simpler cluster expansion holds if we only consider Wightman functions of "in"-fields, namely

$$\langle \Omega, \phi^{\text{in}}(x_1) \cdots \phi^{\text{in}}(x_n) \Omega \rangle = \begin{cases} \sum_{I \in \mathcal{P}'^{(n)}} \prod_{\{j_1, j_2\} \in I} D^+(x_{j_1}, x_{j_2}) & \text{if } n \text{ is even,} \\ 0 & \text{if } n \text{ is odd.} \end{cases} \quad (10)$$

$\mathcal{P}'^{(n)}$ is the collection of all partitions of $\{1, \dots, n\}$ into disjoint subsets containing two elements $\{j_1, j_2\}$ with $j_1 < j_2$, i.e. $\mathcal{P}'^{(n)}$ is a collection of all possible pairings made out of $\{1, \dots, n\}$.

It follows from the Fock construction, (7) and the properties of D^+ that

$$[\phi^{\text{in}}(x), \phi^{\text{in}}(y)] = iD(x, y). \quad (11)$$

Fixing both $\phi^{\text{in}}(x)$ and $\phi^{\text{out}}(x)$ would over-determine the system, therefore we only use (4) as a definition of $\phi^{\text{out}}(x)$ without specifying any further properties of it.

From (3) and (4) it follows immediately that

$$\phi^{\text{out}}(x) = \phi^{\text{in}}(x) + (D * j)(x). \quad (12)$$

Furthermore, because both $\phi^{\text{in}}(x)$ and D fulfill the Klein-Gordon equation, it is already clear at this point that $\phi^{\text{out}}(x)$ does as well. However, we still need to check if the outgoing field fulfills the CCR and find out in what kind of representation it is.

3 Calculation of the Wightman functions

To evaluate Wightman functions we will make use of generalized Feynman graphs. In the following figures we will draw all graphs in ϕ^3 -theory for simplicity unless otherwise stated. However, for the actual calculations the degree p of the ϕ^p -theory is irrelevant. Our calculations will be limited to second order in the loop expansion. However, the calculations can be straightforwardly extended to higher orders in the loop expansion with some more combinatorial effort. We begin developing the graphical calculus by introducing the symbols for the propagators of our theory.

$$D^+(x,y) \cong x \xrightarrow{\text{open}} y \cong D^-(y,x)$$

$$G_r(x,y) \cong x \xrightarrow{\text{double}} y \cong G_a(y,x)$$

$$D(x,y) \cong x \xrightarrow{\text{closed}} y \cong -D(y,x)$$

Figure 1: Propagators

A $D^+(x,y)$ is being represented by a line with an open arrow, a $D(x,y)$ by a line with a closed arrow and a $G_r(x,y)$ by a line with a double open arrow, the arrows pointing to x (see Figure 1).

Next we introduce a tree expansion for the fields according to the Parisi-Wu method [18]. We expand the fields in powers of the coupling constant λ :

$$\phi^a(x) = \sum_{\sigma=0}^{\infty} \lambda^{\sigma} \phi_{\sigma}^a(x). \quad (13)$$

Clearly,

$$\phi_{\sigma}^{\text{in}}(x) = \begin{cases} \phi^{\text{in}}(x) & \text{if } \sigma = 0, \\ 0 & \text{otherwise.} \end{cases} \quad (14)$$

We calculate $\phi_{\sigma}^a(x)$ for $a = \text{loc/out}$ recursively using (4) and (12):

$$\phi_{\sigma}^a(x) = \begin{cases} \phi^{\text{in}}(x) & \text{if } \sigma = 0 \text{ and} \\ \left(\Delta^a * \left(\sum_{\sigma_1, \dots, \sigma_{p-1}=0, \sum \sigma_l=\sigma}^{\infty} \prod_{i=1}^{p-1} \phi_{\sigma_i}^{\text{loc}} \right) \right) (x) & \text{otherwise,} \end{cases} \quad (15)$$

where $\Delta^{\text{loc}} = G_r$, $\Delta^{\text{out}} = D$. Following the recursion in (15), we define tree graphs corresponding to the summands in (15) by an induction over σ . To fix the initial step, we draw field $\phi_0^a(x)$, i.e. an "in"-field, as a leaf attached to a root corresponding to an external x -vertex of type a . A tree corresponding to $\phi_{\sigma}^a(x)$ is drawn by taking $p-1$ trees corresponding to perturbative local fields of order $\sigma_1, \dots, \sigma_{p-1}$ s.t. $\sum \sigma_l = \sigma - 1$, assembling their roots y_1, \dots, y_{p-1} to form a single internal y -vertex and adding a trunk, i.e. a new line from y to x corresponding to a $\Delta^a(x,y)$. Therefore, a tree corresponding to $\phi_{\sigma}^a(x)$ has a root corresponding to an external

x -vertex, a trunk corresponding to a Δ^a , several branches corresponding to G_{rs} , several leaves corresponding to "in"-fields and σ branching points corresponding to internal vertices with a total number of $p-1$ branches and leaves emerging from them. We note that the causal flow (the direction of the G_r -arrows) always points to the root. We label the different tree components inductively, accounting for the fact that the indices σ_i in (15) are distinguishable. The initial step of the induction is fixed by defining the label of a trunk to be the index of the external vertex variable attached to it. To assign a label to a branch/leaf one takes the label of the branch resp. trunk the considered branch/leaf emerges from as a basis. One then extends it by a dot followed by a number reflecting the position of the considered branch/leaf (field) at the actual branching point (in the corresponding current), i.e. the index i of $\phi_{\sigma_i}^{\text{loc}}$ in (15). See Figure 2 for some examples of trees.

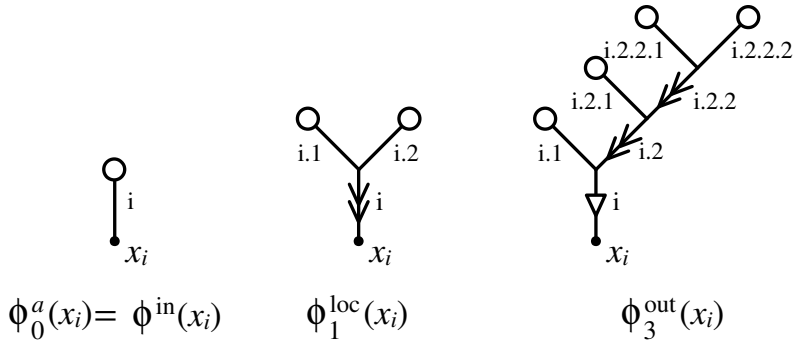


Figure 2: The only possible tree for $\phi_0^a(x)$, the only possible tree for $\phi_1^{\text{loc}}(x)$ and one possible tree for $\phi_3^{\text{out}}(x)$

Now we will proceed with the Wightman functions. To calculate Wightman functions it is sufficient to consider only their connected parts, i.e. the truncated Wightman functions.

In order to calculate the truncated Wightman functions, we will first expand them in powers of the coupling constant λ :

$$\langle \Omega, \phi^{a_1}(x_1) \cdots \phi^{a_n}(x_n) \Omega \rangle^T = \sum_{\sigma=0}^{\infty} \lambda^{\sigma} \langle \Omega, \phi^{a_1}(x_1) \cdots \phi^{a_n}(x_n) \Omega \rangle_{\sigma}^T. \quad (16)$$

Inserting (13) into the left side of (16) and comparing terms of equal order in λ we get:

$$\langle \Omega, \phi^{a_1}(x_1) \cdots \phi^{a_n}(x_n) \Omega \rangle_{\sigma}^T = \sum_{\sigma_1, \dots, \sigma_n=0, \sum \sigma_l=\sigma}^{\infty} \langle \Omega, \phi_{\sigma_1}^{a_1}(x_1) \cdots \phi_{\sigma_n}^{a_n}(x_n) \Omega \rangle^T. \quad (17)$$

We know from the tree expansion that for a fixed σ , every $\phi_{\sigma}^a(x)$ can be expressed in terms of ϕ^{in} s. Therefore it follows that $\langle \Omega, \phi_{\sigma_1}^{a_1}(x_1) \cdots \phi_{\sigma_n}^{a_n}(x_n) \Omega \rangle^T$ can be expressed in terms of Wightman functions of "in"-fields. Finally, using (14), (15), (10) and (17), we can express truncated Wightman functions of arbitrary fields merely in terms of fundamental functions.

We will now introduce Feynman graphs corresponding to perturbative n -point Wightman functions. A Feynman graph of order σ consists of n external vertices corresponding to the arguments x_1, \dots, x_n and type-indices a_1, \dots, a_n of a Wightman function and σ internal vertices

corresponding to arbitrary variables in M . The vertices are connected to the remainder of the graph by q lines, with $q = 1$ ($q = p$) for external (internal) vertices. A line is called an external line if it is connected to an external vertex, an internal line otherwise. While Wightman functions correspond to Feynman graphs, one can show that truncated Wightman functions correspond to connected Feynman graphs. We call a Feynman graph with arrows and labels on all lines an extended Feynman graph.

On the level of graphs, the resolving of (17) via (10) corresponds to gluing the leaves of n trees with a total order of σ together to yield an extended Feynman graph of order σ with n external vertices. As we calculate truncated Wightman functions, only gluing possibilities that yield connected Feynman graphs are allowed.

A line originating from gluing a pair of two leaves together, i.e. a D^\pm -line, is defined to be labeled by combining the leaves' labels to a pair. Starting from the beginning, we compare the two labels slot-by-slot until we find a pair of numbers that does not match. The arrow on the D^\pm -line then points to the leaf corresponding to the lower of those numbers.

We have now described how to expand fields to trees that are subsequently assembled to extended Feynman graphs (see Figure 3 for two examples).

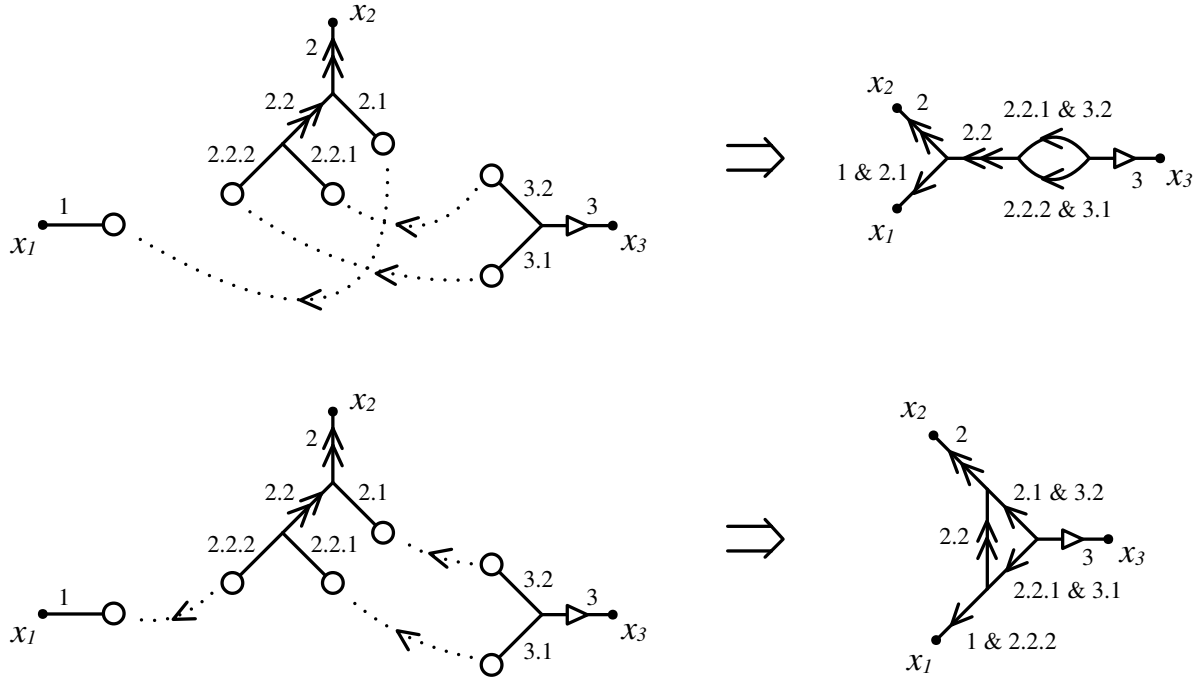


Figure 3: Two possibilities to glue the same set of trees to graphs corresponding to $\langle \Omega, \phi_0^a(x_1) \phi_2^{\text{loc}}(x_2) \phi_1^{\text{out}}(x_3) \Omega \rangle^T$.

This also works the other way round. To calculate $\langle \Omega, \phi^{a_1}(x_1) \cdots \phi^{a_n}(x_n) \Omega \rangle_\sigma^T$, we draw all topologically possible connected Feynman graphs of order σ with n fixed external vertices x_1, \dots, x_n of type a_1, \dots, a_n . We then consider all possibilities to partition each Feynman graph into n connected and loopless subgraphs, i.e. trees, and several remaining lines. Each such subgraph contains exactly one root x_i of type a_i . A partition is fixed by marking a certain number of lines s.t. the Feynman graph with those lines removed consists of n disconnected tree graphs

without leaves, arrows and labels and each internal vertex is part of a such a tree. The external lines connected to external vertices of type $a = \text{in}$ are always marked. Next we assign labels to all external lines according to the indices of their external vertex variables. Using these labels as an initial step and starting from the roots, we walk up the trees on the unmarked lines and inductively assign labels to all lines emerging from the vertices we pass. As a result, the marked lines have two labels, one from each vertex they connect. The inductive dependence of the labels on the preceding labels is fixed by the labeling algorithm defined in the tree expansion above. For each of the possible choices of labels we draw arrows on all lines. The type of the arrows on the unmarked lines is chosen according to a_1, \dots, a_n and the tree expansion. Furthermore,

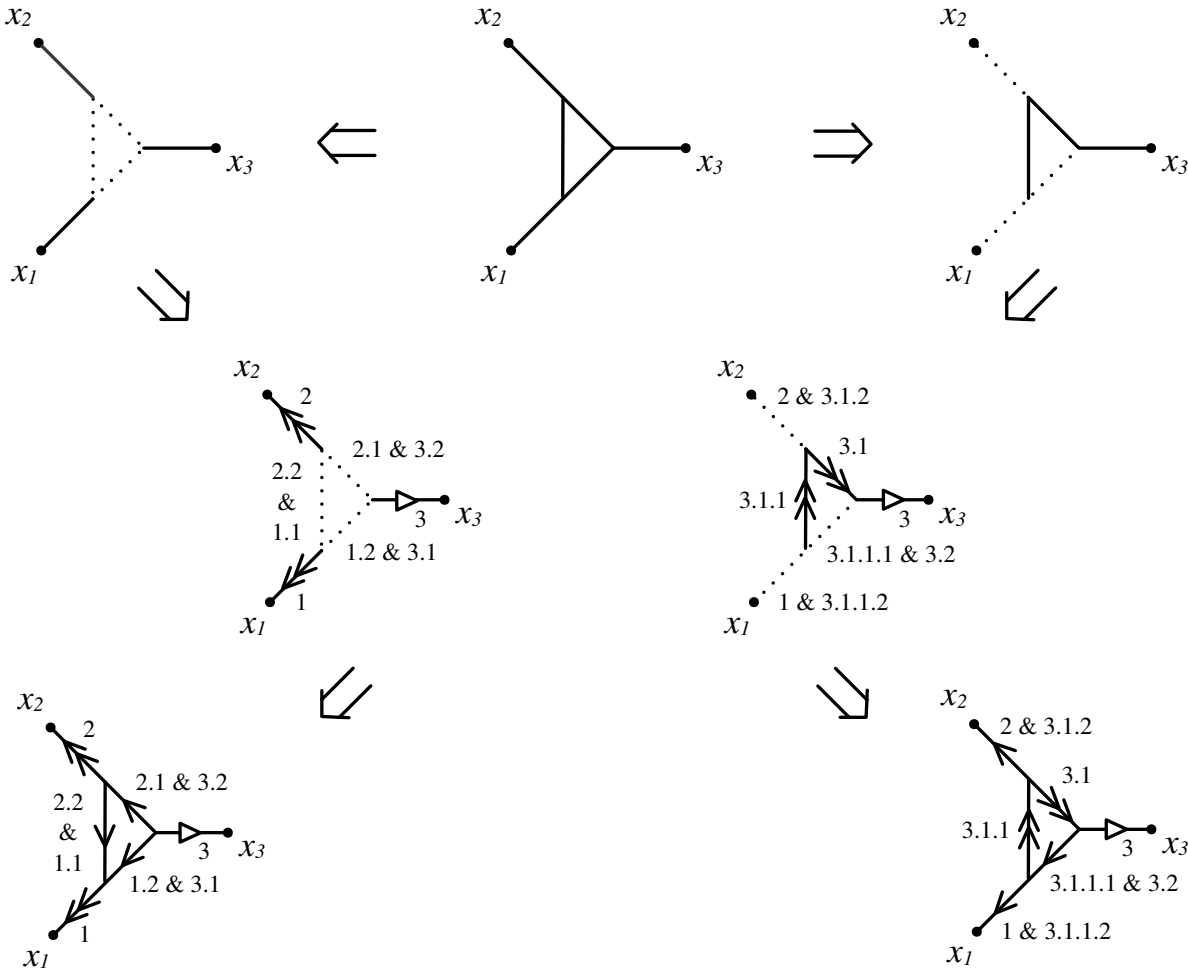


Figure 4: Two possibilities to extend a Feynman graph corresponding to $\langle \Omega, \phi^{\text{loc}}(x_1) \phi^{\text{loc}}(x_2) \phi^{\text{out}}(x_3) \Omega \rangle_3^T$.

each marked line becomes a D^\pm -line. The direction of the arrow on such a line is determined by comparison of the two labels of the line in the manner described in the preceding paragraph.

We call a D^\pm -line a self-gluing line if the numbers in the first slots of its two labels match, a gluing line otherwise. With this definition, a gluing line connects two trees and a self-gluing line connects a leaf-less tree to itself.

To obtain the analytical expression corresponding to an extended Feynman graph, we assign variables to all internal vertices, write down the propagators corresponding to all lines and then integrate over all internal vertices. Once we have the analytical expressions, summing over all topologically possible Feynman graphs and all possibilities to extend them yields $\langle \Omega, \phi^{a_1}(x_1) \cdots \phi^{a_n}(x_n) \Omega \rangle_{\sigma}^T$ (see Figure 4 for two examples).

For the following calculations it is sometimes convenient to drop the labels and replace them by combinatorial factors. In the sum of values corresponding to a certain Feynman graph we will subsume all its extensions with coinciding arrows to a single graph without labels called a reduced Feynman graph. The value of such a reduced graph is defined to be the value of an original extended graph times the number of extended Feynman graphs that give this reduced Feynman graph.

To determine the combinatorial factor of a reduced Feynman graph of order σ from scratch, one first assigns a factor of $(p - 1)!$ (not $p!$ as in commutative Feynman graphs) to each internal vertex yielding a "bare" combinatorial factor of $(p - 1)!\sigma$. Each group of k -fold D^{\pm} -lines connecting the same pair of vertices contributes a factor of $k!^{-1}$. An additional factor of α^{-1} arises from the number α of automorphisms of a reduced Feynman graph, i.e. permutations of internal vertices leaving the graph unchanged [24].

Furthermore, the self-gluing lines of a reduced graph contribute factors as well. To fix these factors we divide the self-gluing lines occurring in graphs up to second order in the loop expansion into three classes and examine them separately. See Appendix A for the details.

In the following two chapters we are merely interested in qualitative results, therefore we will only consider relative combinatorial factors in the sum of values corresponding to a certain Feynman graph.

4 Properties of the Wightman functions: Invariance, Hermiticity, spectral property, positivity

We now want to discuss the fundamental properties of the Wightman functions calculated in Section 3.

Invariance under orthochronous isometric diffeomorphisms As we have shown in Section 3, the Wightman functions of our theory can be expressed in terms of integrals of products of fundamental functions. Since we know from Section 2 that all fundamental functions are invariant under isometric diffeomorphisms preserving the time direction and the integrals contain the canonic volume form which is invariant under all isometric diffeomorphisms by definition, invariance of the Wightman functions follows immediately.

Hermiticity We have to prove

$$\overline{\langle \Omega, \phi^{a_1}(x_1) \cdots \phi^{a_n}(x_n) \Omega \rangle} = \langle \Omega, \phi^{a_n}(x_n) \cdots \phi^{a_1}(x_1) \Omega \rangle. \quad (18)$$

Since we can express the Wightman functions in terms of Wightman functions of "in"-fields convoluted with the real valued fundamental functions $G_{r/a}$ and D and since the order of fields in the latter Wightman function corresponds to the order of fields in the original Wightman function, it is sufficient to prove (18) for $a_1, \dots, a_n = \text{in}$.

We know from (10) how to express Wightman functions of "in"-fields in terms of D^+ . The complex conjugation of (10) exchanges all $D^+(x_{j_1}, x_{j_2})$ with $D^+(x_{j_2}, x_{j_1})$ which obviously corresponds to reversing the total order of fields in the Wightman function of "in"-fields, thus (18) holds for $a_1, \dots, a_n = \text{in}$.

Spectral property In general spacetimes there is no well-defined Fourier transformation, therefore spectral conditions can not be formulated. However, in static spacetimes the time translations form a one parameter group of symmetries and we assume that Fourier transformations w.r.t. the time parameter are possible. A well-defined spectral condition can thus be formulated in that case. On such spacetimes one specifies \tilde{D} with the help of the spectral condition such that the Fourier transform in the time arguments defined by the global timelike killing field of a n -point Wightman functions of "in"-fields vanish if the sums $\sum_{j=l+1}^n E_l$ are not all positive. Here E_l is the variable conjugated to the l -th time argument in the VEV. We note that all fundamental functions are invariant under time translations by our assumptions, hence only depend on time differences of both arguments. Therefore the unitary time translation operator that is obtained from the time translation invariance of Wightman functions via the GNS construction coincides with the time translation operator for the "in"-fields, which has positive spectrum by construction.

Perturbative positivity If we expand Wightman functions perturbatively up to a given order N , we can add further terms of order $\mathcal{O}(\lambda^{N+1})$ to obtain a VEV of fields $\phi^{a,N}(x) = \sum_{\sigma=0}^N \lambda^\sigma \phi_\sigma^a(x)$ that act as operator valued distributions on the "in" Fock space. The VEVs obviously fulfill positivity. Thus, the Wightman functions expanded in λ up to order N fulfill positivity up to a $\mathcal{O}(\lambda^{N+1})$ -term.

5 Properties of the Wightman functions: Locality

To prove locality of the truncated Wightman functions, we have to show that

$$\langle \Omega, \phi^{a_1}(x_1) \dots [\phi^{a_i}(x_i), \phi^{a_{i+1}}(x_{i+1})] \dots \phi^{a_n}(x_n) \Omega \rangle^T \quad (19)$$

vanishes for $x_i \perp x_{i+1}$, $\forall i \in \{1, \dots, n-1\}$, $a_j = \text{loc}$ if $j \in \{i, i+1\}$, $a_j = \text{in/loc/out}$ otherwise.

Up to now, the initial step in our labeling algorithm depended on the index of the respective external vertex variable that in turn corresponded to its position within a Wightman function. If we let $A := \langle \Omega, \phi^{a_1}(x_1) \dots \phi^{a_i}(x_i) \phi^{a_i}(x_{i+1}) \dots \phi^{a_n}(x_n) \Omega \rangle^T$ and $B := \langle \Omega, \phi^{a_1}(x_1) \dots \phi^{a_i}(x_{i+1}) \phi^{a_i}(x_i) \dots \phi^{a_n}(x_n) \Omega \rangle^T$, then for each Feynman graph corresponding to A there exists a topologically identical Feynman graph corresponding to B . It is easy to see that we can label both Feynman graphs in the same way except with i and $i+1$ interchanged in the first slots of all labels. From the algorithm of determining the direction of the arrows on the D^\pm -lines it follows that the arrows on all lines of these two extended Feynman graphs match with the exception that the arrows on the gluing lines connecting the trees with roots x_i & x_{i+1} are reversed. If the two considered graphs do not contain such gluing lines, their values will cancel identically. While calculating (19) we can thus restrict ourselves to extended Feynman graphs with gluing lines connecting the trees with roots x_i & x_{i+1} . Furthermore, because our task will only be to examine if (19) vanishes or not, we will only need to examine the analytical factors corresponding to those lines.

We call a connected subgraph containing only elements of the trees with roots x_i & x_{i+1} and a gluing line connecting those trees a path, if all internal vertices of this subgraph are connected to exactly 2 lines. Following the considerations in the preceding paragraph, while calculating (19) we only need to consider reduced graphs with at least one path. To show that (19) vanishes in the appropriate cases mentioned above, we will subsume all reduced Feynman graphs with topologically equivalent paths and show that each such sum vanishes. If we fix a certain number of topologically possible paths in a Feynman graph, in the process of extending and reducing this graph such that the trees with roots x_i & x_{i+1} are connected by gluing lines, we can vary the position of the gluing and self-gluing lines on these paths without changing the type of (i.e. the arrows on) any line not contained in these paths. Because we are only interested in qualitative results, it is therefore sufficient to consider the contributions of all paths contained in a reduced graph. We will analyze the reduced graphs we calculate by the number l of loops contained in the subgraph one gets by merging all paths.

$$\begin{aligned}
 & \sum_{q=1}^{m+1} \text{Diagram } 1 - \sum_{q=1}^{m+1} \text{Diagram } 2 \\
 &= i \sum_{q=1}^{m+1} \text{Diagram } 3 - i \text{Diagram } 4
 \end{aligned}$$

Diagrams 1, 2, 3, and 4 are Feynman-like graphs with vertices x_i and x_{i+1} at the ends. They consist of a sequence of vertices $u_1, u_{q-1}, u_q, \dots, u_m$ connected by horizontal lines. Vertical lines (gluing lines) connect these vertices to a central vertical line. The arrows on the horizontal lines indicate the direction of flow. Diagram 1 has arrows pointing towards x_i . Diagram 2 has arrows pointing away from x_i . Diagram 3 has arrows pointing towards x_{i+1} . Diagram 4 has arrows pointing away from x_{i+1} .

Figure 5: The case $l = 0$

We start with the most simple case $l = 0$, i.e. reduced graphs containing exactly one path. Let m be the number of vertices on a path. The considered paths only differ in the position of the gluing line, obviously there are $m + 1$ different possible positions. Varying the position of the gluing line on a single path doesn't change the combinatorial factor of a reduced Feynman graph. Summing over all possible positions of the gluing line thus yields a contribution to A of the form

$$\sum_{q=1}^{m+1} \prod_{j=1}^{q-1} G_r(u_{j-1}, u_j) D^+(u_{q-1}, u_q) \prod_{j=q+1}^{m+1} G_a(u_{j-1}, u_j), \quad (20)$$

$u_j, j \in \{1, \dots, m\}$ being the variables of the inner vertices and $u_0 = x_i$, $u_{m+1} = x_{i+1}$. Considering B , we end up with a contribution of the same form, except with $D^+(u_{q-1}, u_q)$ replaced by $D^-(u_{q-1}, u_q)$. Since $D^+ - D^- = iD$, the respective contribution to (19) is of the form

$$i \sum_{q=1}^{m+1} \prod_{j=1}^{q-1} G_r(u_{j-1}, u_j) D(u_{q-1}, u_q) \prod_{j=q+1}^{m+1} G_a(u_{j-1}, u_j). \quad (21)$$

Using (3), we find through "telescope cancelations" that this factor can be expressed as

$$i \left(\prod_{j=1}^{m+1} G_r(u_{j-1}, u_j) - \prod_{j=1}^{m+1} G_a(u_{j-1}, u_j) \right) \quad (22)$$

(see Figure 5). Because of the support properties of $G_{r/a}(x, y)$ the product of the $G_{r/a}(u_{j-1}, u_j)$ can only be non-zero if $u_j \in \overline{V}_{u_{j-1}}^\mp \forall j \in \{1, \dots, m+1\}$ which implies that $u_j \in \overline{V}_{u_s}^\mp \forall j \in \{1, \dots, m+1\}, \forall s \in \{0, \dots, j-1\}$. But this would contradict $x_i \perp x_{i+1}$, therefore the product of the $G_{r/a}$ vanishes if $x_i \perp x_{i+1}$. This shows that under the assumption $x_i \perp x_{i+1}$ the values of extended Feynman graphs with $l = 0$ cancel in the calculation of (19).

Next we will consider reduced Feynman graphs with $l = 1$, i.e. graphs containing exactly 2 paths. The idea is to establish a $G_{r/a}$ -chain on each of the two paths, i.e. to subsume the graphs with $l = 1$ in such a way that the contribution of either of these paths is a factor of the form (22). There are two different types of graphs in this case, graphs with one gluing line (i.e. the trees with roots x_i & x_{i+1} are connected outside the loop) and graphs with two gluing lines (i.e. the trees with roots x_i & x_{i+1} are connected inside the loop). If there is only one gluing line, then one of the lines belonging to the loop must be a self-gluing line. Let $e (f)$ be the number of lines in the loop belonging to the upper (lower) path. Let $ef > 1$. Then there are $e + f$ possibilities for the position of the self-gluing line. For each of those $e + f$ possible cases we will try to establish a $G_{r/a}$ -chain on the path not containing the self-gluing line. Let the self-gluing line be part of the upper path and let $r \in \{1, \dots, e\}$ be the number reflecting its position. In the calculation of (19), the graphs with one gluing line add up to a graph with the gluing line replaced by a D -line and multiplied by i as in the case $l = 0$. To establish a $G_{r/a}$ -chain on the lower path we add graphs with a proper combinatorial factor, an additional factor of i , a self-gluing line on the upper path at position r , a D -line on the lower path at position $s = 1, \dots, q$ and double open arrows pointing to the root "on their side" on the remaining lines of the paths. As in the preceding paragraph, the sum of these graphs yields a $G_{r/a}$ -chain through "telescope cancelations" that vanishes for $x_i \perp x_{i+1}$. After proceeding like this for each of the $e + f$ possible positions of the self-gluing line, we are left with all the graphs with two gluing lines from which we have to subtract all the graphs we have added to establish the $G_{r/a}$ -chains. Since there are $e (f)$ possible positions for a gluing line on the loop belonging to the upper (lower) path, there are ef different types of graphs with two gluing lines (as we have $l = 1$, none of these types can be equivalent through automorphisms). Within the graphs we need to subtract there are also ef types of graphs with a self-gluing line on the upper (lower) path and a D -line on the lower (upper) path. For each $r \in \{1, \dots, e\}$ and $s \in \{1, \dots, f\}$ we sum up the graphs with the two gluing lines at r and s , the graphs with the self-gluing line at r and the D -line at s and the graphs with the D -line at r and the self-gluing line at s (see Figure 6). Since we know from Section 3 and Appendix A that the contributions of the self-gluing lines encountered here are of the form (45) with $k = 1$, the contribution of the two paths in the graphs we are left with is of the form

$$\begin{aligned}
& \left[\frac{1}{2} \left(\begin{array}{c} \text{Diagram 1} \\ \text{Diagram 2} \end{array} \right) + \left(\begin{array}{c} \text{Diagram 3} \\ \text{Diagram 4} \end{array} \right) \right] - \left[\begin{array}{c} \leftarrow \rightarrow \rightarrow \end{array} \right] \\
& + \frac{i}{2} \left[\begin{array}{c} \text{Diagram 5} \\ \text{Diagram 6} \end{array} \right] - C \\
& = \frac{i}{2} \left[\begin{array}{c} \text{Diagram 7} \\ \text{Diagram 8} \\ \text{Diagram 9} \\ \text{Diagram 10} \\ \text{Diagram 11} \\ \text{Diagram 12} \end{array} \right] \\
& + \left[\begin{array}{c} \text{Diagram 13} \\ \text{Diagram 14} \\ - \left(\begin{array}{c} \text{Diagram 15} \\ \text{Diagram 16} \end{array} \right) \\ - \frac{i}{2} \left(\begin{array}{c} \text{Diagram 17} \\ \text{Diagram 18} \\ \text{Diagram 19} \\ \text{Diagram 20} \end{array} \right) \end{array} \right] \\
& = \frac{i}{2} \left[\begin{array}{c} \text{Diagram 21} \\ \text{Diagram 22} \\ \text{Diagram 23} \\ \text{Diagram 24} \\ \text{Diagram 25} \\ \text{Diagram 26} \end{array} \right]
\end{aligned}$$

Figure 6: An example for $l = 1$ with $e = 1$ and $f = 2$

$$\begin{aligned}
& (D^+(u_{r-1}, u_r)D^+(v_{s-1}, v_s) - D^-(u_{r-1}, u_r)D^-(v_{s-1}, v_s)) \\
& - \frac{1}{2}(D^+(u_{r-1}, u_r) + D^-(u_{r-1}, u_r))iD(v_{s-1}, v_s) \\
& - iD(u_{r-1}, u_r)\frac{1}{2}(D^+(v_{s-1}, v_s) + D^-(v_{s-1}, v_s)),
\end{aligned} \tag{23}$$

u_{r-1}, u_r (u_{s-1}, u_s) being the vertices connected by the line on the upper (lower) path at position r (s). Using $iD = D^+ - D^-$ we see that this factor vanishes identically (see Figure 6 for an example). If $e = f = 1$, there is only one possible position for the self-gluing line, as the two paths are topologically equivalent. To treat this case along the same lines as the cases above, we symmetrize the contribution from the self-gluing line over r and s . Since in this case the two occurring gluing lines are connecting the same pair of vertices, they contribute a relative combinatorial factor of 2^{-1} as well, which shows that (23) remains valid for $e = f = 1$.

To proceed with $l = 2$, we need to know all topological possibilities for two loops. To fix these possibilities, we consider a graph with $l = 1$, ignore all lines except those belonging to paths and all vertices except the two branching points of the loop and consider all possibilities to add another line to this graph. To make sure we do not miss any possibility, we proceed in the following way: we identify and name all essential elements of the graph, i.e. the line on the left hand side of the loop γ_1 , the left branching point γ_2 , the upper loop line γ_3 , the lower loop line γ_4 , the right branching point γ_5 and the line on the right hand side of the loop γ_6 (see Figure 7).

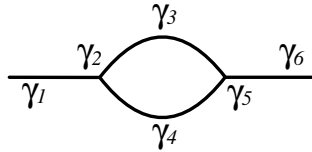


Figure 7: The essential elements of a $l = 1$ graph

We then consider all possibilities to connect two elements γ_i and γ_j by an additional line. $i = j$ is allowed, however, an additional loop attached to the $l = 1$ graph at a single vertex is irrelevant since this additional loop would not be able to contain any gluing lines and therefore this case could be treated as $l = 1$ with an additional irrelevant factor. Following this procedure, we see that the relevant cases with $l = 2$ can be divided into three classes, namely disjoint loops, nested loops and kite graphs. The classes are listed in Figure 8. A dashed line means that both graphs with and without that line are considered to belong to the respective class. Locality can now be shown class by class, cf. Appendix B.

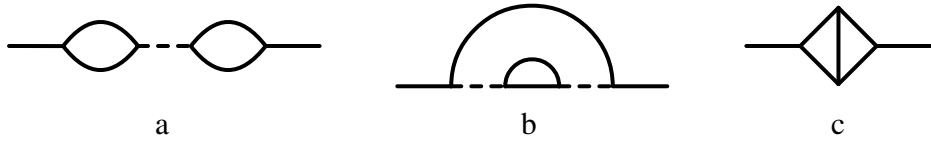


Figure 8: **a)** disjoint loops **b)** nested loops **c)** kite graphs

With help of the methods we have used up to $l = 2$, the cases with $l > 2$ can be calculated straightforwardly under consideration of more complex classes of self-gluing lines.

6 Properties of the "out"-fields

After showing that the Wightman-functions of our theory have all the properties (at least up to second order in the loop expansion) one would demand from a "good" QFT in general spacetimes, we will continue examining the properties of the "out"-fields of our theory.

Klein-Gordon Equation We have already seen in Section 2 that the "out"-fields of our theory fulfill the Klein-Gordon equation.

Canonical commutation relations To prove that the "out"-fields of our theory fulfill the CCR it is necessary and sufficient to show that $[\phi^{\text{out}}(x), \phi^{\text{out}}(y)] = iD(x, y)$ and $\langle \Omega, \phi^{a_1}(x_1) \cdots [\phi^{a_i}(x_i), \phi^{a_{i+1}}(x_{i+1})] \cdots \phi^{a_n}(x_n) \Omega \rangle^T$ vanishes for all $n > 2$, $\forall i \in \{1, \dots, n\}$, $a_j = \text{out}$ if $j \in \{i, i+1\}$, $a_j = \text{in/loc/out}$ otherwise. [11, Lemma 5.2]

To show this we follow the same lines as in the proof of the locality of the Wightman functions. We again only need to consider graphs with at least one path. In these cases we again try to establish chains similar to the $G_{r/a}$ -chains, but we have to account for the fact that the trunk-propagators $G_r(u_0, u_1)$ and $G_r(u_{m+1}, u_m)$ in (21) are being replaced by D s yielding

$$\begin{aligned} & iD(x_i, u_1) \left(\prod_{j=2}^m G_a(u_{j-1}, u_j) - \prod_{j=2}^m G_r(u_{j-1}, u_j) \right. \\ & \left. + \sum_{q=2}^m \prod_{j=2}^{q-1} G_r(u_{j-1}, u_j) D(u_{q-1}, u_q) \prod_{j=q+1}^m G_a(u_{j-1}, u_j) \right) D(u_m, x_{i+1}), \end{aligned} \quad (24)$$

if $m > 1$, where we have separated the terms with $q = 1$ and $q = m + 1$ from the sum and accounted for the antisymmetry of $D(x, y)$. Using (3), we find through "telescope cancelations" that the remaining terms of the sum over q equal the separated terms but with the opposite sign, so (24) vanishes identically. If $m = 1$, replacing the trunk-propagators $G_r(u_0, u_1)$ and $G_r(u_{m+1}, u_m)$ in (21) by D s, yields

$$iD(u_0, u_1)D(u_2, u_1) + iD(u_0, u_1)D(u_1, u_2) \quad (25)$$

which vanishes identically because of the antisymmetry of D . If $m = 0$, which is obviously only possible for $n = 2$, no trunk-propagators occur and the only possible graph consists of one gluing line, thus (21) with $m = 0$ equals the truncated 2-point Wightman function of "out"-fields, yielding

$$\langle \Omega, [\phi^{\text{out}}(x), \phi^{\text{out}}(y)] \Omega \rangle^T = iD(x, y) = [\phi^{\text{out}}(x), \phi^{\text{out}}(y)]. \quad (26)$$

Representation One of the main claims of this article is that in general the CCR representation of the "out"-field is *not* quasifree.

To see this, let us consider d -dimensional Minkowski spacetime with metric $g(\epsilon) = (1 + \epsilon h)\eta$ where η is the Minkowski metric and h a C^∞ -function of compact support. To first order in λ in ϕ^4 theory, the only non-vanishing n -point function for the "out"-field is due to the star graph. Due to telescope cancelations, cf. [11], one obtains

$$\lambda \times \text{Im} \int_{\mathbb{R}^d} \prod_{l=1}^4 D_{g(\epsilon)}^-(x_j, x) (1 + \epsilon h)^{d/2} dx \quad (27)$$

Expanding to first order in ϵ , we obtain two sorts of contributions: One from the expansion of $(1 + \epsilon h)^{d/2}$ and four terms from the first order expansion of the D_g^- .

Fourier transforming on Minkowski space-time, we see that the support of the first contribution w.r.t. k_1, \dots, k_4 is on the negative shell in all four energy-momentum variables k_j . Furthermore, it is non-vanishing since the delta distribution that is obtained from the integration in the case $\epsilon = 0$ in the first order term is replaced with the Fourier transform of h , which is

non-vanishing and can be seen as the consequence of energy-momentum violation in the quantum system due to the gravitational field. Taking the imaginary part amounts to subtracting the same expression with D^- replaced by D^+ and division by i . Both terms have disjoint support and can not cancel each other.

The first order contribution to $D_{g(\epsilon)}^-(x)$ is easily calculated to be $(d/2)G_r * [\eta^{ab}(\partial_a h) \times \partial_b D^-](x)$. When the Fourier transform is carried out, the product between the derivative of h and the derivative of D^- leads to a term that is off-shell. For the second type of contribution to (27) thus three of the momenta k_j are on the negative shell and the fourth is off-shell. Energy-momentum conservation holds, i.e. $k_1 + \dots + k_4 = 0$, as the integration is carried out w.r.t. the flat measure.

Apparently, both types of contributions in the first order calculation have disjoint support and thus (27) is really non vanishing.

To see that this implies the non vanishing of higher order truncated n -point functions at higher orders of perturbation theory we refer to the following (non-rigorous) consideration: Due to the symmetry of the higher order functions it is enough to focus on VEVs of $\phi^{\text{out}}(f) = \int_M \phi(x)f(x)d_gx$ for some fixed f such that the truncated four point contribution is non-vanishing. Due to positivity and as there always exists a solution to the Hamburger moment problem, VEVs of powers of $\phi(f)$ form the moments of a probability distribution that has a non-vanishing fourth cumulant. It is well-known from probability theory that this implies that higher order even cumulants can not be vanishing either, from which it follows that the higher order truncated Wightman functions are not identically zero.

7 Unitary transformations between CCR representations

Given a quasifree representation of the CCR with Fock-space \mathcal{F} , in this section we calculate the particle content of non-quasifree representations that are unitarily equivalent to the given quasifree one. In the following section we then apply this result to the "out"-state CCR that we have calculated. Here we use the language of Wightman functionals and \star -calculus, cf. Appendix C for a short introduction.

Let $\varphi(x)$ be the operator valued distribution fulfilling the Klein-Gordon equation and the CCR that has been obtained via the GNS-construction from some Wightman functional \underline{W}' with GNS space \mathcal{F}_{GNS} and GNS vacuum $\Psi_0 \in \mathcal{F}_{\text{GNS}}$. Let $\xi(x)$ be the operator valued distribution obtained from the quasifree Wightman functional \underline{W} via the Fock construction given in Section 2 with $\Omega \in \mathcal{F}$ the Fock vacuum. The relevant application will of course be $\varphi = \phi^{\text{out}}$ and $\xi = \phi^{\text{in}}$, cf. the next section. We assume unitary equivalence of both CCR representations in the following technical sense: Let $U : \mathcal{F}_{\text{GNS}} \rightarrow \mathcal{F}$ be a unitary transformation such that $U\varphi(f)U^* = \xi(f)$ for all test functions and let $\Psi = U\Psi_0 \in \mathcal{F}$ such that Ψ is in a dense core of some closure of the Fock creation and annihilation operators $a(\psi)$ and $a^\dagger(\chi)$, $\psi \in \mathcal{H}^+$, $\chi \in \mathcal{H}^-$. It is furthermore assumed that for any vector Υ in this core, the vectors $a^\sharp(\psi_1) \dots a^\sharp(\psi_n)\Upsilon$ are jointly continuous in the ψ_l w.r.t. the $(\mathcal{H}^\pm)^{\otimes n}$ and the \mathcal{F} topologies, where a^\sharp stands for a or a^\dagger .

To determine U , it is enough to calculate Ψ , since $U\varphi(f_1) \dots \varphi(f_n)\Psi_0 = \xi(f_1) \dots \xi(f_n)\Psi$, $f_l \in \mathcal{D}(M)$, can be calculated using (6), once the n -particle components of Ψ are known.

As a state in \mathcal{F} , Ψ can be parameterized as

$$\Psi = \sum_{n=0}^{\infty} \int_{M^{\times n}} f_n(x_1, \dots, x_n) \xi(x_1) \cdots \xi(x_n) d_g x_1 \cdots d_g x_n \quad (28)$$

where the complex functions f_n are symmetric under permutation of arguments and purely positive frequency, i.e. $(K^-)^{\otimes n} (\tilde{D}^*)^{\otimes n} f_n = 0$, and fulfill a normalization condition, $\|\Psi\|_{\mathcal{F}}^2 = \sum_{n=0}^{\infty} \|(\tilde{D}^*)^{\otimes n} f_n\|_{\mathcal{H}^{\otimes n}}^2 = 1$. Here (\tilde{D}^*) is the operator that acts by convolution with \tilde{D} . Furthermore, the f_n are taken from some function space s.t. $f_n \mapsto (\tilde{D}^*)^{\otimes n} f_n \in \mathcal{H}^{\otimes n}$ is onto. Let $\underline{f} = (f_0, f_1, f_2, \dots)$, then obviously

$$\underline{W}' = \overrightarrow{D}_{\underline{f}^*} \overleftarrow{D}_{\underline{f}} \underline{W} = \sum_{n,j=0}^{\infty} \overrightarrow{D}_{f_n^*} \overleftarrow{D}_{f_j} \underline{W} \quad (29)$$

where the convergence of the infinite sums on the right hand side follows from the assumption that Ψ is in a core for the *closed* creation and annihilation operators. Application of (52) and \star -multiplication with $\underline{W}^{-1} = \exp_{\star}(-\underline{W}^T)$ yields

$$\begin{aligned} \exp_{\star}(\underline{W}'^T - \underline{W}^T) &= \sum_{m,j=0}^{\infty} \int_{M^{\times(n+j)}} \sum_{\substack{I \in \mathcal{P}(\{1, \dots, n+j\}) \\ I = \{I_1, \dots, I_k\}, k \geq 1}} \star_{l=1}^k \overleftrightarrow{D}_{I_l} \underline{W}^T \\ &\quad \times f_n^*(x_1, \dots, x_n) f_j(x_{n+1}, \dots, x_{n+j}) d_g x_1 \cdots d_g x_{n+j} \end{aligned} \quad (30)$$

Both, \underline{W}' and \underline{W} induce CCR representations. By [11, Lemma 5.2] this is equivalent to $\text{Im} D^+ = \text{Im} \underline{W}_2^T = \frac{1}{2} D$ and $\underline{W}_n^T(x_1, \dots, x_n)$ is symmetric under permutation of arguments – and hence real by the Hermiticity of \underline{W}' – for $n \geq 3$. This automatically holds for the quasifree state \underline{W} since $\underline{W}_2^T = D^+$ and $\underline{W}_n^T(x_1, \dots, x_n) = 0$ for $n \geq 3$. Hence the left hand side of (30) is real and symmetric. We note that

$$\left. \begin{aligned} \overleftrightarrow{D}_{I_l} \underline{W}^T &= 0 && \text{for } |I_l| > 3 \\ \overleftrightarrow{D}_{I_l} \underline{W}^T &= (D^+(x_{j_1}, x_{j_2}), 0, \dots) && \text{for } I_l = \{j_1, j_2\}, j_1 < j_2 \\ \overrightarrow{D}_{I_l} \underline{W}^T &= (0, D^+(x_j, \cdot), 0, \dots) && \text{for } I_l = \{j\} \\ \overleftarrow{D}_{I_l} \underline{W}^T &= (0, D^+(\cdot, x_j), 0, \dots) && \text{for } I_l = \{j\} \end{aligned} \right\}. \quad (31)$$

Thus only those partitions in (30) contribute that consists of sets with one or two elements, only. Given such a partition $I = \{I_1, \dots, I_l\}$, let $S = \cup_{l:|I_l|=1} I_l$ and $\hat{I} \in \mathcal{P}'(\{1, \dots, n+j\} \setminus S)$ the remainder, which is a pairing partition. We get

$$\sum_{\substack{I \in \mathcal{P}(\{1, \dots, n+j\}) \\ I = \{I_1, \dots, I_k\}, k \geq 1}} \star_{l=1}^k \overleftrightarrow{D}_{I_l} \underline{W}^T = \sum_{\substack{S \subseteq \{1, \dots, n+j\} \\ \hat{I} \in \mathcal{P}'(\{1, \dots, n+m\} \setminus S) \\ \hat{I} = \{I_1, \dots, I_{(n+j-|S|)/2}\} \\ I_l = \{i_l, j_l\}, i_l < j_l}} \prod_{l=1}^{(n+j-|S|)/2} D^+(x_{i_l}, x_{j_l}) \star_{j \in S} \overleftrightarrow{D}_{x_j} \underline{W}^T. \quad (32)$$

Clearly, $(\star_{j \in S} \overleftrightarrow{D}_{x_j} \underline{W}^T)_s = 0$ if $s \neq |S|$ and for $s = |S|$, $S = \{j_1, \dots, j_s\}$, $j_1 < j_2 < \dots < j_q \leq n < j_{q+1} < \dots < j_s$

$$\left(\star_{j \in S} \overleftrightarrow{D}_{x_j} \underline{W}^T\right)_s (y_1, \dots, y_s) = \sum_{\pi \in \text{Perm}(s)} \prod_{l=1}^q D^+(x_{j_l}, y_{\pi(l)}) \prod_{l=q+1}^s D^-(x_{j_l}, y_{\pi(l)}). \quad (33)$$

Inserting (32) and (33) into (31) yields

$$\begin{aligned} \exp_{\star} \left(\underline{W}'^T - \underline{W}^T \right)_s (y_1, \dots, y_s) &= \sum_{\substack{r \geq s \\ r-s \text{ even}}} \sum_{n=0}^r \int_{M^{\times r}} \sum_{\substack{\{j_1, \dots, j_s\} \subseteq \{1, \dots, r\} \\ j_1 < \dots < j_q \leq n \\ < j_{q+1} < \dots < j_s}} \sum_{\substack{\hat{I} \in \mathcal{P}'(\{1, \dots, n+m\} \setminus S) \\ \hat{I} = \{I_1, \dots, I_{(r-s)/2}\} \\ I_l = \{i_l, k_l\}, i_l < k_l}} \sum_{\pi \in \text{Perm}(s)} \\ &\quad \times \prod_{l=1}^{(r-s)/2} D^+(x_{i_l}, x_{k_l}) \prod_{l=1}^q D^+(x_{j_l}, y_{\pi(l)}) \prod_{l=q+1}^s D^-(x_{j_l}, y_{\pi(l)}) \\ &\quad \times f_n^*(x_1, \dots, x_n) f_{r-n}(x_{n+1}, \dots, x_r) d_g x_1 \cdots d_g x_r. \end{aligned} \quad (34)$$

We note that $\int_M D^{\pm}(x, y) f(x) d_g x = 0$ if f is positive/negative frequency, cf. (6). Furthermore, f_n^* is purely negative frequency and f_{n-r} purely positive frequency. One can thus replace all propagator functions D^{\pm} in (34) by the real symmetric function $\tilde{D} = D^+ + D^-$, since the integral over the added propagator D^{\mp} with f_n^* or f_{n-r} always vanishes.

Having done so, we can commute the sums over n and over S on the right hand side of (34), s.t. the integral contains the function

$$\tilde{z}_r(x_1, \dots, x_r) = \sum_{n=0}^r f_n^*(x_1, \dots, x_n) f_{n-r}(x_{n+1}, \dots, x_r). \quad (35)$$

The next step is to symmetrize, $z_r(x_1, \dots, x_r) = (r!)^{-1} \sum_{\pi \in \text{Perm}(r)} \tilde{z}_r(x_{\pi(1)}, \dots, x_{\pi(r)})$, which also makes z_r a real function, and to replace \tilde{z}_r by z_r . In fact, let $1 \leq j < r$, then we have to show that \tilde{z}_r is integrated w.r.t. a function which is symmetric in x_j and x_{j+1} . Given one term in the combinatorial sum, suppose that $j, j+1 \in S$. Then symmetry follows from summation over $\text{Perm}(s)$. Next suppose that either j or $j+1$ is in a pairing and the other index is in S . Then there exists another contribution to the combinatorial sum where j and $j+1$ are exchanged showing symmetry for this case. Let finally j and $j+1$ both be in a pairing. If the pairings are different, the argument just given applies. If this is one and the same pairing, then symmetry follows from the symmetry of \tilde{D} .

Taking into account that the sum over $\text{Perm}(s)$ accounts for a factor $s!$, the sum over S for a factor $\binom{r}{s}$ and the sum over pairings for a factor $2^{s-r}(r-s)!/((r-s)/2)!$, one obtains a combinatorial factor $c_{s,r}$ by multiplication of these contributions. This finally leads to

$$\begin{aligned} \exp_{\star} \left(\underline{W}'^T - \underline{W}^T \right)_s (y_1, \dots, y_s) &= \sum_{\substack{r=s \\ r-s \text{ even}}}^{\infty} c_{s,r} \int_{M^{\times r}} \prod_{l=1}^{(r-s)/2} \tilde{D}(x_{2l-1}, x_{2l}) \\ &\quad \times \prod_{l=r-s+1}^r \tilde{D}(x_l, y_{l-r+s}) z_r(x_1, \dots, x_r) d_g x_1 \cdots d_g x_r. \end{aligned} \quad (36)$$

$$\begin{aligned}
1 &= \text{○} = c_{0,0} \text{○} + c_{0,2} \text{○} \leftarrow \rightarrow + c_{0,4} \text{○} \leftarrow \leftarrow \rightarrow \rightarrow + c_{0,6} \text{○} \leftarrow \leftarrow \leftarrow \rightarrow \rightarrow \dots \\
\text{○} &= c_{2,2} \text{○} \leftarrow \leftarrow \rightarrow \rightarrow + c_{2,4} \text{○} \leftarrow \leftarrow \leftarrow \rightarrow \rightarrow + c_{2,6} \text{○} \leftarrow \leftarrow \leftarrow \leftarrow \rightarrow \rightarrow \dots \\
\text{○} &= c_{4,4} \text{○} \leftarrow \leftarrow \leftarrow \rightarrow \rightarrow + c_{4,6} \text{○} \leftarrow \leftarrow \leftarrow \leftarrow \rightarrow \rightarrow \dots \\
&\vdots \qquad \qquad \qquad \vdots
\end{aligned}$$

Figure 9: The triangular system of equations for the functions $(\tilde{D}*)^{\otimes r} z_r$

We want to solve this system of equations for the solution part of z_r , i.e. for $(\tilde{D}*)^{\otimes r} z_r$. To understand (36) better, we denote the s -point function of the functional on the left hand side by a white circle with s legs and the function z_r by a shaded circle with r amputated legs. The integrations w.r.t. the propagators \tilde{D} then adds either free legs that carry two arrows with opposite direction, cf. Figure 12 in Appendix A, or a line of that type that goes back into the shaded circle. $(\tilde{D}*)^{\otimes r} z_r$ thus corresponds to the shaded circle with r legs with double arrows of opposite direction. One so obtains two decoupled systems, one for s even and one for s odd, cf. Figure 7 for the even system, which makes the upper triangular structure visible. In the following we focus on solving the even system, the odd system can be solved alike. In ϕ^p -theories with p even, the odd system is identically zero on the left hand side and hence gives $(\tilde{D}*)^{\otimes r} z_r = 0$ for odd r . We note that the empty circles are solutions of the Klein-Gordon equation in each of their legs. By the demand of continuity of the creation/annihilation operators in ψ and χ when repeatedly applied to Ψ , we find by Riesz' lemma that the empty circle with s legs is in $\mathcal{H}^{\hat{\otimes} s}$. Let $\{h_j\}_{j \in \mathbb{N}}$ be a ONS in \mathcal{H} . Taking the scalar product with h_j in the first two legs and then summing over j on the right hand side induces an opposite double arrow line that goes back into the shaded circle, since $(\tilde{D} * f, \tilde{D} * h) = \tilde{D}(f, h)$ for f, h real. On the left hand side we denote this contraction operation by a arrow-less line going back into the white circle.

The unique solution of the even system can thus be written down in graphical form as in Figure 10. The solution exists by assumption of unitary equivalence, thus all infinite sums involved in the inverse system converge, which follows from $\lim_{n \rightarrow \infty} \Pi(n)\Psi = \Psi$ in \mathcal{F} where $\Pi(n)$ projects on states with at most n particles and the fact that for a state with at most n particles we have a finite system of equations. The constants $d_{s,r}$ are defined as the entries of the inverse of the upper triangular matrix $C = (c_{s,r})_{s,r \in 2\mathbb{N}}$.

It remains to reconstruct the solution part of the functions f_n , $(\tilde{D}*)^{\otimes n} f_n$, from the functions $(\tilde{D}*)^{\otimes r} z_r$. These functions are solutions of the Klein-Gordon equation in each argument. Let us first suppose that $z_0 = |f_0|^2 \neq 0$. As the state Ψ is only determined up to a phase, one may

Figure 10: Solution to the triangular system

assume $f_0 > 0$. Then by (35)

$$(K^+)^{\otimes r}(\tilde{D}*)^{\otimes r}z_r(x_1, \dots, x_r) = f_0(\tilde{D}*)^{\otimes r}f_r(x_1, \dots, x_r), \quad \text{for } r \in \mathbb{N}. \quad (37)$$

If $(\tilde{D})^{\otimes r}z_r = 0$ for $r < r_0$ and r_0 is maximal, r_0 must be even. It follows that $(\tilde{D})^{\otimes n}f_n = 0$ for $n < r_0/2$. There exist $y_1, \dots, y_{r_0/2} \in M$ such that $(K^-)^{\otimes \frac{r_0}{2}} \otimes (K^+)^{\otimes \frac{r_0}{2}}(\tilde{D}*)^{\otimes r_0}z_{r_0}(y_1, \dots, y_{r_0/2}, y_1, \dots, y_{r_0/2}) = |(\tilde{D}*)^{\otimes \frac{r_0}{2}}f_{r_0/2}(y_1, \dots, y_{r_0/2})|^2 > 0$. We may fix the phase such that $(\tilde{D}*)^{\otimes \frac{r_0}{2}}f_{r_0/2}(y_1, \dots, y_{r_0/2}) > 0$ and we obtain the solution part of f_n , $n \geq r_0/2$, via

$$\begin{aligned} & (K^-)^{\otimes \frac{r_0}{2}} \otimes (K^+)^{\otimes \frac{r_0}{2}+n}(\tilde{D}*)^{\otimes \frac{r_0}{2}+n}z_{\frac{r_0}{2}+n}(y_1, \dots, y_{r_0/2}, x_1, \dots, x_n) \\ &= (\tilde{D}*)^{\otimes \frac{r_0}{2}}f_{r_0/2}(y_1, \dots, y_{r_0/2})(\tilde{D}*)^{\otimes n}f_n(x_1, \dots, x_n). \end{aligned} \quad (38)$$

8 The three S -matrices

In this section we give a detailed account on the scattering behavior of quantum fields on curved spacetimes. We do this under the assumption that there are preferred, quasifree "in"- and "out"-representations of the CCR and that the preferred "in"-representation is the one chosen for the incoming field $\phi^{\text{in}}(x)$. These preferred representations can e.g. be found for manifolds that are asymptotically static for the past and the future. In this case they can be determined via the spectral condition. We furthermore restrict to the case where all these three representations are unitarily equivalent, i.e. to physical situations where the average number of quantum particles produced by gravitational forces is finite.

We then have three different CCR representations for the free field, namely the "in"-Fock representation with field operator $\phi^{\text{in}}(x)$, Fock vacuum $\Omega = \Omega^{\text{in}}$ and Fock space \mathcal{F}^{in} , the in general non-quasifree "out"-representation with field operator $\phi^{\text{out}}(x)$, GNS-vacuum Ψ_0 (which can be chosen to be Ω as we are in the Heisenberg picture) and GNS-representation Hilbert space

\mathcal{F}_{GNS} and the preferred "out"-Fock representation with field operator $\zeta^{\text{out}}(x)$, Fock-vacuum Ω^{out} and Fock space \mathcal{F}^{out} .

The complete scattering matrix $S : \mathcal{F}^{\text{in}} \rightarrow \mathcal{F}^{\text{out}}$ can then be decomposed as follows

$$S = RUV \quad \mathcal{F}^{\text{in}} \xrightarrow{R} \mathcal{F}_{\text{GNS}} \xrightarrow{U} \mathcal{F}^{\text{in}} \xrightarrow{V} \mathcal{F}^{\text{out}} \quad (39)$$

The first S -matrix R is the quantum scattering one and it is determined by

$$\langle \phi^{\text{in}}(f_1) \cdots \phi^{\text{in}}(f_n) \Omega, R\phi^{\text{in}}(h_1) \cdots \phi^{\text{in}}(h_j) \Omega \rangle = \langle \Omega, \phi^{\text{in}}(\bar{f}_n) \cdots \phi^{\text{in}}(\bar{f}_1) \phi^{\text{out}}(h_1) \cdots \phi^{\text{out}}(h_j) \Omega \rangle, \quad (40)$$

where $f_1, \dots, f_n, h_1, \dots, h_j \in \mathcal{D}(M)$. The right hand side can be calculated using the Feynman rules of Section 3.

In the next step we are free to make a choice: Using the results of Section 7, we can either determine the matrices UV at once or just determine U . We choose the latter possibility since firstly this makes clear the difference to the existing literature [1, 2, 3, 5] and secondly the inverse system of equations in this case only contains finitely many equations and can be solved easily. In fact, for the N -th order perturbation theory in λ in ϕ^p theory all empty circles with more than Np legs on the right hand side of Figure 10 vanish.

The last S -matrix V can now be determined by the calculation of the vacuum associated with a Bogoliubov transform, cf. Section 7. We go through this standard construction very quickly, mainly in order to adapt it to our notation, and refer to [22] for the details: As unitary equivalence implies that the scalar products on the entire solution space induced by the quasifree preferred "in"- and "out"-representation are equivalent, we can consider the projection maps $K_{\text{in}/\text{out}}^{\pm}$ as maps on one Hilbert space $\mathcal{H} = \mathcal{H}_{\text{out}}^+ \oplus \mathcal{H}_{\text{out}}^- = \mathcal{H}_{\text{in}}^+ \oplus \mathcal{H}_{\text{in}}^-$. With

$$\left. \begin{array}{ll} A = K_{\text{in}}^+|_{\mathcal{H}_{\text{out}}^+} : \mathcal{H}_{\text{out}}^+ \rightarrow \mathcal{H}_{\text{in}}^+ & \bar{A} = K_{\text{in}}^-|_{\mathcal{H}_{\text{out}}^-} : \mathcal{H}_{\text{out}}^- \rightarrow \mathcal{H}_{\text{in}}^- \\ B = K_{\text{in}}^-|_{\mathcal{H}_{\text{out}}^+} : \mathcal{H}_{\text{out}}^+ \rightarrow \mathcal{H}_{\text{in}}^- & \bar{B} = K_{\text{in}}^+|_{\mathcal{H}_{\text{out}}^-} : \mathcal{H}_{\text{out}}^- \rightarrow \mathcal{H}_{\text{in}}^+ \\ C = K_{\text{out}}^+|_{\mathcal{H}_{\text{in}}^+} : \mathcal{H}_{\text{in}}^+ \rightarrow \mathcal{H}_{\text{out}}^+ & \bar{C} = K_{\text{out}}^-|_{\mathcal{H}_{\text{in}}^-} : \mathcal{H}_{\text{in}}^- \rightarrow \mathcal{H}_{\text{out}}^- \\ E = K_{\text{out}}^-|_{\mathcal{H}_{\text{in}}^+} : \mathcal{H}_{\text{in}}^+ \rightarrow \mathcal{H}_{\text{out}}^- & \bar{E} = K_{\text{out}}^+|_{\mathcal{H}_{\text{in}}^-} : \mathcal{H}_{\text{in}}^- \rightarrow \mathcal{H}_{\text{out}}^+ \end{array} \right\} \quad (41)$$

one obtains the defining relations for Bogoliubov transforms

$$\left. \begin{array}{lll} A^*A - B^*B = \mathbf{1} & A^*\bar{B} - B^*\bar{A} = 0 & A^* = C \\ C^*C - E^*E = \mathbf{1} & C^*\bar{E} - E^*\bar{C} = 0 & \bar{B}^* = -E \end{array} \right\}. \quad (42)$$

Unitary equivalence on the level of creation and annihilation operators of the fields in the preferred "in"- and "out"-representations is

$$Va_{\text{in}}(\chi)V^* = a_{\text{out}}(\bar{C}\chi) - a_{\text{out}}^\dagger(\bar{E}\chi), \quad Va_{\text{in}}^\dagger(\psi)V^* = a_{\text{out}}^\dagger(C\psi) - a_{\text{out}}(E\psi), \quad \chi \in \mathcal{H}_{\text{in}}^-, \psi \in \mathcal{H}_{\text{in}}^+. \quad (43)$$

We also recall that by the mapping $\chi \mapsto (\bar{\chi}, \cdot)_{\mathcal{H}_{\text{out}}^+}$ one can naturally identify $\mathcal{H}_{\text{out}}^-$ with the dual of $\mathcal{H}_{\text{out}}^+$. Let now $\mathcal{E} = \bar{E}\bar{C}^{-1} : \mathcal{H}_{\text{out}}^- \rightarrow \mathcal{H}_{\text{out}}^+$. Shales theorem implies that $\mathcal{E}^*\mathcal{E}$ is trace-class. Then $\mathcal{H}_{\text{out}}^- \otimes \mathcal{H}_{\text{out}}^- \ni \chi \otimes \psi \mapsto (\bar{\chi}, \mathcal{E}\psi)_{\mathcal{H}_{\text{out}}^+}$ defines a bi-continuous (here Shale's condition enters), linear map on $\mathcal{H}_{\text{out}}^- \otimes \mathcal{H}_{\text{out}}^-$ and thus, by Riesz' lemma, an element ε of $(\mathcal{H}_{\text{out}}^+)^{\otimes 2}$ which in fact is in the symmetric tensor space $(\mathcal{H}_{\text{out}}^+)^{\hat{\otimes} 2}$ as $\bar{\mathcal{E}}^* = \mathcal{E}$. One then obtains the following explicit representation of the transformed vacuum

$$V\Omega = c(1, 0, \sqrt{\frac{1}{2}}\varepsilon, 0, \sqrt{\frac{3 \cdot 1}{4 \cdot 2}}\varepsilon^{\hat{\otimes} 2}, 0, \dots). \quad (44)$$

where $\hat{\otimes}$ is the symmetrized tensor product and c is a normalization constant such that $V\Omega$ has unit norm.

A Combinatorial factors of self-gluing lines

In this appendix we examine the different classes of self-gluing lines occurring in second order loop approximation graphs (see Figure 11 for examples).

The first class contains k -fold ($k > 1$) dependent self-gluing lines, i.e. in the process of extending a Feynman graph, fixing the direction of the arrow on one of the lines by comparing its pair of labels immediately fixes the direction of the arrows on the other $k - 1$ lines. In other words, if we denote by q the number of steps after which the algorithm of fixing the arrow on one of these lines terminates, then the pair of labels of all these k lines match in the first q slots. k is chosen to be maximal, i.e. there is no other self-gluing line correlated to the k lines in the described way.

The second class contains k -fold ($k > 1$) self-gluing lines that are equivalent in the sense that they can be permuted without changing the reduced graph and independent in terms of a correlation described in the previous class. k is again chosen to be maximal in an obvious way.

The third and last class contains single self-gluing lines, i.e. all self-gluing lines that are not correlated or equivalent to any other self-gluing line.

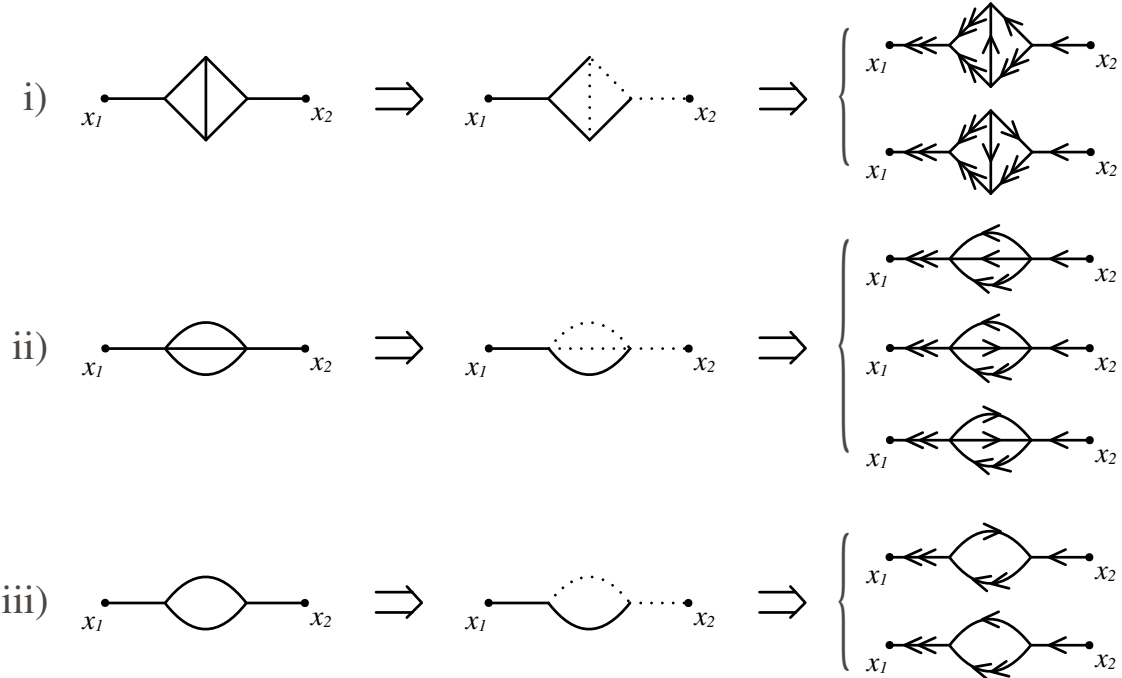


Figure 11: i) An example of a group of two dependent self-gluing lines; ii) an example of a group of two equivalent self-gluing lines, we had to draw a ϕ^4 graph this time since equivalent self-gluing lines do not occur in ϕ^3 -theory; iii) an example of a single self-gluing line.

If a partitioned Feynman graph does not have any self-gluing lines, all possibilities to label it yield the same extended graph and therefore can be subsumed into a single reduced graph. If a partitioned Feynman graph contains one maximal group of k self-gluing lines (with $k = 1$ for single lines), different possibilities to label the graph may yield different possibilities for the directions of the arrows on the k lines, i.e. different extended Feynman graphs. If we let b be the number of the latter possibilities, it is easy to see that a partitioned Feynman graph with one maximal group of k self-gluing lines yields b reduced graphs with a combinatorial factor of b^{-1} relative to the combinatorial factor of the reduced graph originating from a topologically equivalent partitioned Feynman graph without self-gluing lines. It follows that each maximal group of k self-gluing lines contributes a reducing combinatorial factor of b^{-1} . It remains to fix b in dependence of k and the class of the lines.

In general, $b = 2$ for self-gluing lines of the first and third class. If $b = 1$, there is only one possibility for the direction of the arrows on the k lines, because all k pairs of vertices connected by these lines can be permuted at once by an automorphism of the graph. In this case we symmetrize the directions of the arrows which lets us treat these cases as if $b = 2$. It follows that each group of self-gluing lines of the first and third class contributes a total factor of the form

$$\frac{1}{2} \left(\prod_{j=1}^k D^+(u_j, v_j) + \prod_{j=1}^k D^-(u_j, v_j) \right). \quad (45)$$

We will draw single self-gluing lines as lines with two single open arrows showing in opposite directions for convenience (see Figure 12).

$$\tilde{D}(x, y) = D^+(x, y) + D^-(y, x) \cong x \bullet\bullet y$$

Figure 12: The propagator symbol for a single self-gluing line

Furthermore, $b = k + 1$ for self-gluing lines of the second class. Each group of self-gluing lines of this class contributes a total factor of the form

$$\frac{1}{k+1} \sum_{i=0}^k \prod_{j=1}^k D^{s_{ji}}(u_j, v_j); \quad s_{ji} = \begin{cases} + & \text{if } j \leq k-i, \\ - & \text{otherwise.} \end{cases} \quad (46)$$

B $l = 2$ in detail

In this appendix it is convenient to simplify our reduced graphs. We draw only lines belonging to paths and drop all vertices except the branching points of the loops. A line with a certain arrow type in a simplified graph corresponds to the sum over all chains of a fixed number of $m + 1$ ($m \geq 0$) lines in the original reduced graph containing a line with the same arrow and m additional $G_{r/a}$ -lines. In case of a D^{\pm} -, D - and \tilde{D} -line, the double arrows of the additional $G_{r/a}$ -lines point away from that line, in case of $G_{r/a}$ -line the double arrows of the additional

$G_{r/a}$ -lines point into the same direction as the double arrow on that line. We draw simplified $G_{r/a}$ -lines without any arrows or drop them if they are not important. Self-gluing lines are drawn as crossed lines if their class is unclear. To avoid confusion with normal graphs, we will draw all simplified graphs with bold lines.

Disjoint loops As in the case $l = 1$ we have graphs with one and two gluing lines. The graphs with one gluing line (1GL) again add up to graphs with a D -line instead of the gluing line. Obviously there are four different paths in this case. Following the procedure used for $l = 1$ we establish $G_{r/a}$ -chains on each of these paths by adding and subtracting graphs with a self-gluing line and a $G_{r/a}$ -line on one loop and a D -line and a self-gluing line on the other loop. Again it remains to show that the 2GL graphs and the subtracted graphs with a D -line cancel. To do so, we fix one of the loops to contain an upper/lower $G_{r/a}$ -line and a lower/upper self-gluing line. Then the remaining graphs with that loop containing these lines add up to zero as in the case $l = 1$. One such cancellation is depicted in Figure 13. The other three are obtained by flipping each graph in Figure 13 horizontally and/or vertically without changing the direction of the arrows. If one loop consists of a double line, i.e. $m = 0$ for both lines of that loop, one symmetrises as in the case $l = 1$ and then proceeds as described above.

$$\text{Diagram 13: } \text{Graph 1} - \text{Graph 2} - \frac{1}{2} \text{Graph 3} - \frac{1}{2} \text{Graph 4} = 0$$

Figure 13: One cancellation in the calculation of disjoint loops

Nested loops In general, we have 1GL, 2GL and 3GL graphs. The possible positions of self-gluing lines in 1GL graphs are depicted in Figure 14. The self-gluing lines in the last graph of Figure 14 are dependent self-gluing lines while the self-gluing lines in the other graphs are single self-gluing lines.



Figure 14: The possible positions of self-gluing lines in 1GL graphs with two nested loops

For all possible positions of self-gluing lines in the 1GL graphs we add and subtract graphs with appropriate D -lines on the path not containing any self-gluing lines to establish a $G_{r/a}$ -chain on this path.

The possible 2GL graphs are depicted in Figure 15. Each of the four pairs cancels with the

$$\left[\text{Diagram 1} \quad \text{Diagram 2} \quad \text{Diagram 3} \quad \text{Diagram 4} \right] - \left[\text{Diagram 5} \quad \text{Diagram 6} \quad \text{Diagram 7} \right]$$

Figure 15: The possible 2GL graphs with two nested loops

two subtracted graphs that have a D -line and a single self-gluing line at the position of its two gluing lines analogously to the case $l = 1$, see Figure 16 for an example.

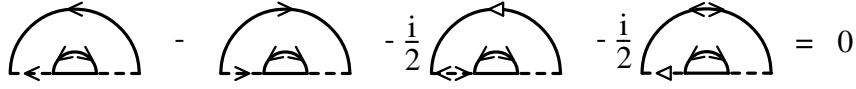


Figure 16: One cancellation of 2GL graphs in the calculation of nested loops

The pair of 3GL graphs cancels with the remaining subtracted graphs as depicted in Figure 17.

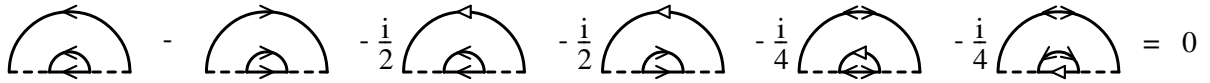


Figure 17: The cancellation of the 3GL graphs in the calculation of nested loops

If the inner loop consists of a double line, we symmetrize as in the previous cases. If both dashed lines are absent and all three other lines are lines with $m = 0$, i.e. we have a triple line connecting the same pair of vertices, we need to calculate separately. In this case, the 1GL graphs contain two equivalent self-gluing lines. We add and subtract the appropriate graphs to establish a $G_{r/a}$ -chain together with the 1GL graphs. The 3GL graphs then cancel with the subtracted graphs, cf. Figure 18.

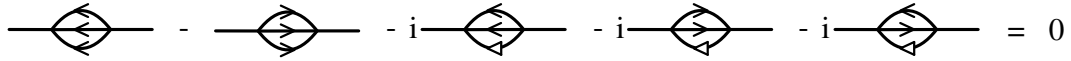


Figure 18: The cancellation of the 3GL graphs in the calculation of triple-line loops

The graphs are in Figure 18 are summed up without a relative combinatorial factor since the 3GL graphs have a reducing factor of $3!^{-1}$ and the 1GL a factor of 3^{-1} from the class of self-gluing lines and a factor of 2^{-1} because the two self-gluing lines connect the same pair of vertices.

Kite graphs We start as in the case of nested loops. We first note that we have 1GL, 2GL and 3GL graphs and consider all possible positions of self-gluing lines in 1GL graphs, cf. Figure 19.

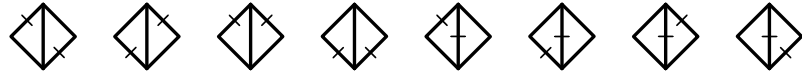


Figure 19: The possible positions of self-gluing lines in 1GL kite graphs

The first four graphs in Figure 19 contain single self-gluing lines. The last four graphs contain dependent or single self-gluing lines depending on the position of the gluing line relative to the two loops, cf. Figure 20 for an example.

$$\frac{1}{2} \leftarrow \begin{array}{c} \diagup \\ \diagdown \end{array} \rightarrow + \frac{1}{2} \leftarrow \begin{array}{c} \diagdown \\ \diagup \end{array} \rightarrow \leftarrow \begin{array}{c} \diagup \\ \diagdown \end{array} \rightarrow \Rightarrow \frac{1}{4} \leftarrow \begin{array}{c} \diagup \\ \diagdown \end{array} \rightarrow$$

Figure 20: An example for the dependence of the class of self-gluing lines on the relative position of the gluing line in 1GL kite graphs

To establish $G_{r/a}$ -lines on the paths not containing any self-gluing lines it is thus not sufficient to add and subtract graphs with D -lines, but also necessary to add and subtract 1GL graphs with single self-gluing lines to "replace" the graphs with dependent self-gluing lines.

The 1GL graphs with dependent self-gluing lines add up with the subtracted 1GL graphs with single self-gluing lines to graphs with D -lines on the position of the self-gluing lines, an example is depicted in Figure 21.

$$\frac{i}{2} \leftarrow \begin{array}{c} \diagup \\ \diagdown \end{array} \rightarrow + \frac{i}{2} \leftarrow \begin{array}{c} \diagdown \\ \diagup \end{array} \rightarrow - \frac{i}{4} \leftarrow \begin{array}{c} \diagup \\ \diagdown \end{array} \rightarrow = \frac{i^3}{4} \leftarrow \begin{array}{c} \diagup \\ \diagdown \end{array} \rightarrow$$

Figure 21: An example for the sum of 1GL kite graphs with dependent self-gluing lines and subtracted 1GL kite graphs with single self-gluing lines

For all four graphs similar to the one on the right hand side of Figure 21 we resolve the D -line outside the loop into $G_{r/a}$ -lines. We can resolve a simplified D -line into $G_{r/a}$ -lines analogously as in original reduced graphs through "telescope cancelations". We observe that one half of the graphs we get in this way contain a $G_{r/a}$ -chain that is known to vanish. We resolve the remaining D -line of the other half of the graphs into $G_{r/a}$ -lines and subsume them to yield the graphs depicted in Figure 22.

$$\frac{i^3}{4} \left[\leftarrow \begin{array}{c} \diagup \\ \diagdown \end{array} \rightarrow - \leftarrow \begin{array}{c} \diagdown \\ \diagup \end{array} \rightarrow - \leftarrow \begin{array}{c} \diagup \\ \diagdown \end{array} \rightarrow + \leftarrow \begin{array}{c} \diagdown \\ \diagup \end{array} \rightarrow \right]$$

Figure 22: The remaining contribution of 1GL graphs in the calculation of kite graphs

Figure 23 shows the possible 2GL graphs.

$$\left[\begin{array}{c} \diagup \\ \diagdown \end{array}, \begin{array}{c} \diagdown \\ \diagup \end{array}, \begin{array}{c} \diagup \\ \diagdown \end{array}, \begin{array}{c} \diagdown \\ \diagup \end{array}, \begin{array}{c} \diagup \\ \diagdown \end{array}, \begin{array}{c} \diagdown \\ \diagup \end{array} \right] - \left[\leftarrow \rightarrow \right]$$

Figure 23: The possible 2GL kite graphs

As in the nested loop case they cancel with the subtracted graphs with a D -line and a single self-gluing line at the position of their gluing lines.

The 3GL graphs add up with the remaining subtracted graphs to graphs with D -lines at the position of the three gluing lines. After resolving two of these D -lines into $G_{r/a}$ -lines and subsuming all graphs we are left with the graphs shown in Figure 24.

$$\begin{aligned}
& \left[\begin{array}{c} \text{graph} \\ \text{graph} \end{array} \right] - \left[\begin{array}{c} \text{graph} \\ \text{graph} \end{array} \right] \\
& - \frac{i}{4} \left[\begin{array}{c} \text{graph} \\ \text{graph} \\ \text{graph} \\ \text{graph} \\ \text{graph} \\ \text{graph} \end{array} \right] \\
& = \frac{i^3}{4} \left[\begin{array}{c} \text{graph} \\ \text{graph} \end{array} \right] \\
& = \frac{i^3}{4} \left[\begin{array}{c} \text{graph} \\ \text{graph} \\ \text{graph} \end{array} \right] - \frac{i^3}{4} \left[\begin{array}{c} \text{graph} \\ \text{graph} \\ \text{graph} \end{array} \right]
\end{aligned}$$

Figure 24: The contribution of 3GL kite graphs and subtracted graphs with D -lines that do not cancel with 2GL graphs

Four of the graphs in the last row of Figure 24 cancel with the four graphs in Figure 22. The remaining two graphs contain closed $G_{r/a}$ -chains. From the discussion of $G_{r/a}$ -chains in Section 5 we know that the closed chains are only non-vanishing if the variables at all their vertices match. But in this case $G_r = G_a$ for all lines contained in the two loops and therefore the analytical expression of the D -line vanishes.

C \star -calculus

In this appendix we present some useful applications of \star -calculus, that goes back to Borchers [6] and Ruelle [19], for a more recent work putting \star -calculus for quantum fields in the context of Hopf algebras see e.g. Maeste and Oeckl [16].

Let $\underline{\mathcal{D}}$ be the Borchers's algebra with multiplication \otimes and unit $\mathbf{1} = (1, 0, \dots)$, i.e. the non-commutative, unital, involutive, topological, free tensor algebra over the space of complex valued test functions $\mathcal{D}(M)$, (M, g) being the manifold under consideration. If $\underline{f} \in \underline{\mathcal{D}}$ is a monomial, $\underline{f} = (0, \dots, 0, f_n, 0, \dots)$ then we identify \underline{f} with $f_n \in \mathcal{D}(M^{\times n})$. We also note that the involution \star acts via $f_n^*(x_1, \dots, x_n) = \overline{f_n(x_n, \dots, x_1)}$. For $f_j \in \mathcal{D}(M)$ and $N \subset \mathbb{N}$ finite, we define $\otimes_{j \in N} f_j$ ($\otimes_{\emptyset} f_j = \mathbf{1}$) where the tensor product preserves the natural order of N . A co-commutative co-product $\Delta : \underline{\mathcal{D}} \rightarrow \underline{\mathcal{D}} \otimes \underline{\mathcal{D}}$ is defined by

$$\Delta(\otimes_{n \in N} f_n) = \sum_{S \subseteq N} (\otimes_{n \in S} f_n) \otimes (\otimes_{n \in N \setminus S} f_n) \quad (47)$$

and linear, continuous extension. Note that in (47) the tensor products in the parentheses are multiplication in $\underline{\mathcal{D}}$, whereas the tensor product between the parentheses is the one in $\underline{\mathcal{D}} \otimes \underline{\mathcal{D}}$. Furthermore, the projection $\varepsilon((f_0, f_1, \dots)) = f_0$ defines a co-unit.

Let $\underline{\mathcal{D}}' = \{(W_0, W_1, \dots) : W_0 \in \mathbb{C}, W_n \in \mathcal{D}'(M^{\times n}), n \geq 1\}$ be the topological dual of $\underline{\mathcal{D}}$, i.e. the space of Wightman functionals. In many applications, a Wightman functional will be given by the sequence of n -point (truncated) VEVs, i.e. $W_n^{(T)}(x_1, \dots, x_n) = \langle \Omega, \varphi(x_1) \cdots \varphi(x_n) \Omega \rangle^{(T)}$

for some operator valued distribution φ . The co-product on $\underline{\mathcal{D}}$ naturally leads to a product, \star , making $\underline{\mathcal{D}}'$ a commutative algebra with unit $\mathbf{1} = \varepsilon$, $\underline{W} \star \underline{V} = (\underline{W} \otimes \underline{V}) \circ \Delta$.

From (47) we get

$$(\underline{W} \star \underline{V})_{|N|}(\otimes_{n \in N} f_n) = \sum_{S \subseteq N} W_{|S|}(\otimes_{n \in S} f_n) V_{|N|-|S|}(\otimes_{n \in N \setminus S} f_n) \quad (48)$$

which shows the coincidence with Borchers' s -product.

It is easy to see that $(\underline{W}^{\star n})_m = 0$ for $n > m$ and $\underline{W} \in \underline{\mathcal{D}}'_1 = \{\underline{V} \in \underline{\mathcal{D}}' : V_0 = 0\}$. Hence, arbitrary \star -power series converge on $\underline{\mathcal{D}}'_1$. In particular, \star -exponential $\exp_{\star} : \underline{\mathcal{D}}'_1 \rightarrow \mathbf{1} + \underline{\mathcal{D}}'_1$ and \star -logarithm $\log_{\star} : \mathbf{1} + \underline{\mathcal{D}}'_1 \rightarrow \underline{\mathcal{D}}'_1$ are well defined through their power series $\exp(t) = \sum_{n=0}^{\infty} t^n / n!$ and $\log(t) = -\sum_{n=1}^{\infty} (1-t)^n / n$. Furthermore, the \star -exp and log functions are inverses of each other and the usual relations hold, i.e. $\exp_{\star}(\underline{W} + \underline{V}) = \exp_{\star} \underline{W} \star \exp_{\star} \underline{V}$, $\exp_{\star}(0) = \mathbf{1}$ and $\log_{\star}(\underline{W} \star \underline{V}) = \log_{\star} \underline{W} + \log_{\star} \underline{V}$. For $\log_{\star} \underline{W}$ we also use the notation \underline{W}^T . In fact, for \underline{W} the collection of Wightman functions, W_n^T is the truncated n -point function defined in equation (9) above, cf. [6].

Let $f \in \mathcal{D}(M)$, and $\vec{m} (f), \overleftarrow{m} (f) : \underline{\mathcal{D}} \rightarrow \underline{\mathcal{D}}$ be the left and right multiplication with f in $\underline{\mathcal{D}}$. We then define left and right derivatives \vec{D}_f and \overleftarrow{D}_f on $\underline{\mathcal{D}}'$ via $\vec{D}_f \underline{W} = \underline{W} \circ \vec{m} (f)$ and $\overleftarrow{D}_f \underline{W} = \underline{W} \circ \overleftarrow{m} (f)$. In fact, it is easily verified that

$$\vec{D}_f (\underline{W} \star \underline{V}) = (\vec{D}_f \underline{W}) \star \underline{V} + \underline{W} \star (\vec{D}_f \underline{V}) \quad (49)$$

where \vec{D}_f stands either for \vec{D}_f or for \overleftarrow{D}_f . This implies for a formal power series $h(t)$ that $\vec{D}_f h_{\star}(\underline{W}) = h'_{\star}(\underline{W}) \star \vec{D}_f \underline{W}$. For notational convenience we sometimes write $\vec{D}_f = \int_M f(x) \vec{D}_x d_g x$

Higher order derivative operators $\vec{D}_f \underline{W} = \underline{W} \circ \vec{m} (f)$, $f \in \underline{\mathcal{D}}$, can also be written as $\vec{D}_f = \sum_{n=0}^{\infty} \vec{D}_{f_n}$, and for f_n symmetric under permutation of arguments

$$\vec{D}_{f_n} = \int_{M^{\times n}} f(x_1, \dots, x_n) \vec{D}_{x_1} \cdots \vec{D}_{x_n} d_g x_1 \cdots d_g x_n. \quad (50)$$

By induction it is easy to see that for f_n and f_j symmetric the following chain rule holds

$$\begin{aligned} \vec{D}_{f_n} \vec{D}_{f_j} h_{\star}(\underline{W}) &= \sum_{k=1}^{n+j} h_{\star}^{(k)}(\underline{W}) \star \int_{M^{\times(n+j)}} \sum_{\substack{I \in \mathcal{P}(\{1, \dots, n+j\}) \\ I = \{I_1, \dots, I_k\}}} \star_{l=1}^k \vec{D}_{I_l} \underline{W} \\ &\quad \times f_n(x_1, \dots, x_n) f_j(x_{n+1}, \dots, x_{n+j}) d_g x_1 \cdots d_g x_{n+j}, \end{aligned} \quad (51)$$

where $\mathcal{P}(N)$ is the set of partitions of N and $\vec{D}_{I_l} = \vec{D}_{x_{j_1}} \cdots \vec{D}_{x_{j_q}} \overleftarrow{D}_{x_{s_1}} \cdots \overleftarrow{D}_{x_{s_r}}$ for $I_l = \{j_1, \dots, j_q, s_1, \dots, s_r\}$, $1 \leq j_1 < j_2 < \dots < j_q \leq n < s_1 < s_2 < \dots < s_r \leq n+j$.

For $h(t) = \exp(t)$, $\underline{W}^T \in \underline{\mathcal{D}}'_1$ and $\underline{W} = \exp_{\star}(\underline{W}^T)$ we finally obtain

$$\begin{aligned} \vec{D}_{f_n} \vec{D}_{f_j} \underline{W} &= \underline{W} \star \int_{M^{\times(n+j)}} \sum_{\substack{I \in \mathcal{P}(\{1, \dots, n+j\}) \\ I = \{I_1, \dots, I_k\}, k \geq 1}} \star_{l=1}^k \vec{D}_{I_l} \underline{W}^T \\ &\quad \times f_n(x_1, \dots, x_n) f_j(x_{n+1}, \dots, x_{n+j}) d_g x_1 \cdots d_g x_{n+j}. \end{aligned} \quad (52)$$

Acknowledgements: For the first named author it is a pleasure to thank Horst Thaler for the ongoing and very fruitful exchange of ideas.

References

- [1] N. D. Birrell, Momentum space renormalization of $\lambda\phi^4$ in curved space–time, *J. Phys. A: Math. Gen.* **13** (1980), 569–584.
- [2] N. D. Birrell, P. C. W. Davies, *Quanum fields in curved space*, Cambridge University Press, Cambridge 1982.
- [3] N. D. Birrell, P. C. W. Davies, L. H. Ford, Effects of field interactions upon particle creation in Robertson-Walker universes, *J.Phys. A: Math. Gen.* **13**, 901–908 (1980).
- [4] N. D. Birrell, L.H. Ford, Self-interacting quantized fields and particle creation in Robertson-Walker universes, *Annals Phys. (N.Y.)* **122**, 1–25 (1979).
- [5] N. D. Birrel, J. G. Taylor, Analysis of interacting quantum field theory in curved spacetime, *J.Math. Phys.* **21** No. 7, 1740–1760 (1980).
- [6] H. J. Borchers, H. J. Algebraic aspects of Wightman quantum field theory. International Symposium on Mathematical Problems in Theoretical Physics (Kyoto Univ., Kyoto, 1975), pp. 283–292. Lecture Notes in Phys., 39. Springer, Berlin, 1975.
- [7] R. Brunetti, K. Fredenhagen, Microlocal analysis and interacting quantum field theories: Renormalization on physical backgrounds, *Commun.Math.Phys.* **208**, 623–661 (2000).
- [8] R. Brunetti, K. Fredenhagen, M. Köhler, The microlocal spectrum condition and Wick polynomials on curved spacetimes, *Commun. Math. Phys.* **180**, 633–652 (1996).
- [9] T. S. Bunch, P. Pangangaden, L. Parker, On renormalization of $\lambda\phi^4$ field theory in curved spacetime: I, *J. Phys. A: Math. Gen.* **13**, 901–932 (1980).
- [10] J. Dimock, Algebras of local observables on a manifold, *Commun. Math. Phys.* **77**, 219–228 (1980).
- [11] H. Gottschalk H. Thaler, An Indefinite Metric Model for Interacting Quantum Fields on Globally Hyperbolic Space-Times, *Ann. H. Poincaré*, **4**, 637–659 (2003).
- [12] S. Hollands, W. Rual, The state space of perturbative quantum field theory in curved space times, *Ann. H. Poincaré* **3** No. 4, 635–657 (2002).
- [13] S. Hollands, R. M. Wald, Local wick polynomials and time ordered products of quantum fields in curved spacetime, *Commun. Math. Phys.* **223**, 289–326 (2001).
- [14] S. Hollands, R. M. Wald, Existence of local covariant time ordered products of quantum fields in curved spacetime, *Commun. Math. Phys.* **231** 309–345 (2002).
- [15] S. Hollands, R. M. Wald, On the renormalization group in curved spacetime, *Commun. Math. Phys.* **237** 123–160 (2003).
- [16] A. Mestre, R. Oeckl, Combinatorics of n -point functions via Hopf algebras in quantum field theory, *J. Math. Phys.* **47** (2006), 052301, math-ph/0505066.

- [17] A. Ostendorf, Feynman rules for Wightman functions, Ann. Inst. H. Poincare **40** No. 3, 273–290 (1984).
- [18] G. Parisi, Wu Y.-S., Perturbation theory without gauge fixing, Sci. Sinica **24** No. 4, 483–496 (1981).
- [19] D. Ruelle, Statistical mechanics: rigorous results, Benjamin, Massachusetts 1969.
- [20] O. Steinmann, Perturbation theory for Wightman functions, Commun.Math. Phys **152**, 627–645 (1993)
- [21] O. Steinmann, Perturbative quantum electrodynamics and axiomatic field theory, Springer Verlag, Berlin/Heidelberg/New York, 2000.
- [22] R.M. Wald, Quantum field theory in curved space-time and black hole thermodynamics, Chicago Univ. Press 1993.
- [23] C.N. Yang, D. Feldman, The S -Matrix in the Heisenberg representation, Phys. Rev. **79**, 972-987 (1950).
- [24] W. Zimmerman, Local Operator Products and Renormalization in Quantum Field Theory, *Lectures on Elementary Particle Physics and Quantum Field Theory*, Brandeis University, Summer Institute in Theoretical Physics; MIT Press, Cambridge (1970).

HANNO GOTTSCHALK

Institut für angewandte Mathematik

Wegelerstr. 6

D-51373 Bonn, Germany

e-mail: gottsch@wiener.iam.uni-bonn.de

THOMAS HACK

Physikalisches Institut

Nußallee 12

D-51373 Bonn, Germany

e-mail: tommeck@tommeck.com